Molecular Biology of the Cell
Vol. 16, 3832–3846, August 2005

# Stat3 Is Required for Full Neoplastic Transformation by the Simian Virus 40 Large Tumor Antigen

**Adina Vultur,* Rozanne Arulanandam,* James Turkson,† Guilian Niu,† Richard Jove,† and Leda Raptis***

*Departments of Microbiology and Immunology and Pathology, Queen's University, Kingston, Ontario K7L 3N6, Canada; and †H. Lee Moffitt Cancer Center, University of South Florida, Tampa, FL 33612

Submitted December 22, 2004; Revised April 18, 2005; Accepted May 18, 2005
Monitoring Editor: Gerard Evan

**To investigate the role of Stat3 (signal transducer and activator of transcription-3) in neoplastic transformation by the Large Tumor antigen of Simian Virus 40 (TAg), murine fibroblasts were rendered deficient in Stat3 activity through expression of a Stat3-specific siRNA or a Cre-loxP recombination system. The results demonstrate that growth rate, formation of foci overgrowing a monolayer of normal cells and colony formation in soft agar were dramatically reduced in Stat3-deficient cells. In addition, TAg expression led to increased Stat3 tyrosine phosphorylation, DNA binding, and transcriptional activity, suggesting that Stat3 is required for TAg-mediated neoplasia. Stat3 activation was prevented by blocking the binding of TAg to pRb (retinoblastoma-susceptibility gene product), whereas genetic ablation of pRb increased Stat3 activity, suggesting that pRb inactivation by TAg might be responsible for the observed Stat3 activation. Stat3 activation by TAg was suppressed after inhibition of c-Src, JAKs or the insulin-like growth factor receptor. On the other hand, targeted disruption of the Fer kinase or pharmacological inhibition of Abl had no effect. Inhibition of Src activity led to Stat3 down-regulation as well as apoptosis of sparsely growing, TAg-transformed cells. However, Src inhibition was relatively ineffective in confluent cells, consistent with previous results indicating that cell to cell adhesion activates Stat3 by a Src-independent mechanism. Direct Stat3 inhibition on the other hand induced apoptosis very effectively in confluent cells, which could have significant therapeutic implications. Taken together, our results suggest that Stat3 is an important component of a pathway emanating from TAg and leading to neoplastic conversion.**

## INTRODUCTION

The Simian Virus 40 large Tumor antigen (TAg) is a multifunctional oncoprotein capable of neoplastically transforming a variety of mammalian cell types (Sullivan and Pipas, 2002). This transforming competence is thought to result from its ability to activate a combination of several different mechanisms to override cellular growth controls. Such mechanisms include the interaction with two tumor-suppressor proteins, p53 (Sullivan and Pipas, 2002) and the retinoblastoma-susceptibility gene product (pRb; Chau and Wang, 2003).

The signal transducer and activator of transcription (STAT) proteins were initially discovered as key mediators of cytokine signaling (reviewed in Levy and Darnell, Jr., 2002; Yu and Jove, 2004). Later studies demonstrated that the STAT proteins are also activated by receptor tyrosine kinases such as the receptors for the epidermal growth factor (EGF) or platelet-derived growth factor (PDGF; EGFR and PDGFR, respectively), or the nonreceptor tyrosine kinase Src (Turkson *et al.*, 1998; Bromberg *et al.*, 1998; Vignais and Gilman, 1999; Wang *et al.*, 2000). STATs are invariably latent in the cytoplasm and, subsequent to binding to an activated receptor through their SH2 domains, STATs become activated through phosphorylation by the receptor itself or by the associated JAK or c-Src tyrosine kinases. Phosphorylation of a single critical tyrosine residue activates STATs by stabilizing the association of two STAT monomers through reciprocal SH2-ptyr interactions to form a dimer which migrates to the nucleus and binds specific DNA sites to initiate transcription from a number of genes. Seven distinct STAT proteins have so far been identified in mammalian cells (Yu and Jove, 2004). Signaling through Stat3 is determined by a key phosphorylation at tyr705.

Previous results demonstrated that TAg activates the Ras/Raf/Erk pathway (Raptis *et al.*, 1997a; Grammatikakis *et al.*, 2001). Given that the Ras and Stat3 pathways are often coordinately regulated by growth factors or oncogenes, we examined whether, in addition to Ras, TAg might also be able to activate Stat3. Our previous findings also revealed that cell-cell adhesion causes a dramatic increase in Stat3 activity in both normal and transformed cells (Vultur *et al.*, 2004); hence, the effect of TAg upon Stat3 activity was examined at different levels of confluence. The data indicate that TAg expression results in increased phosphorylation of Stat3 at the crucial tyr-705 site, as well as stimulation of Stat3 DNA binding and transcriptional activity at all levels of confluence examined. Moreover, Stat3 down-regulation through genetic ablation, or transfection with dominant-negative mutants or siRNA, abrogated the ability of TAg to induce colony formation in soft agar or formation of foci overgrowing a monolayer. These results indicate that Stat3 activity is necessary for full neoplastic transformation by TAg.

Analysis of TAg functions required for Stat3 activation suggested a role for the pRb-binding site on TAg. In addi-

This article was published online ahead of print in *MBC in Press* (http://www.molbiolcell.org/cgi/doi/10.1091/mbc.E04–12–1104) on May 25, 2005.

Address correspondence to: Leda Raptis (raptisl@post.queensu.ca).



© 2005 by The American Society for Cell Biology

tion, cells from mice with a targeted disruption of the *Rb* gene had high levels of Stat3 activity compared with their wild-type counterparts. These findings are consistent with the possibility that pRb inactivation by TAg plays a role in the TAg-mediated, Stat3 activation. Examination of the nature of tyrosine kinases involved indicated that Stat3 activation by TAg was suppressed following inhibition of c-Src, Jaks, or IGF1R but not inhibition of the Fer or Abl tyrosine kinases. Furthermore, although inhibition of Src could induce apoptosis in sparse, TAg-transformed cells, it was relatively ineffective in dense cultures, consistent with our previous finding indicating that the density-mediated, Stat3 activation is independent from c-Src action. In contrast, direct inhibition of Stat3 could induce apoptosis more effectively in confluent cells. Taken together, our data indicate that Stat3 may be an integral component of signaling pathways emanating from nuclear oncogenes, which lead to neoplasia.

## MATERIALS AND METHODS

### *Cell Lines, Culture Techniques, and Gene Expression*

Tissue culture medium (DMEM) was from ICN (Aurora, OH) and calf serum from Life Technologies (Burlington, Ontario, Canada). Normal mouse NIH 3T3, and NIH 3T3 transformed by v-Src (Zhang *et al.,* 2000), mouse 10T½ and rat F111 fibroblasts have been previously described (Raptis *et al.,* 1997a) and were grown in plastic dishes in DMEM supplemented with 10% calf serum, in a 7% $CO_2$ incubator. Fibroblasts established from mice with a targeted disruption of Jak2 were a kind gift of Dr. E. Parganas and Dr. J. Ihle and maintained in DMEM with 10% fetal calf serum (FCS).

For treatment with the AG490 JAK inhibitor, cells were incubated with 50 $\mu$M AG490 for a total of 1–8 d, with redosing every 12 h as described (Zhang *et al.,* 2000). Treatment with the PD180970 Src inhibitor was at a final concentration of 0.2 $\mu$M, with redosing every 12 h for a total of 24 h at all time points before lysis, as described in *Results.* Treatment with the SU6656 Src inhibitor was at 5 $\mu$M for 24 h. Treatment with STI571 (imatinib or Gleevec, a generous gift from Dr. Buchdunger of Novartis) was for up to 48 h at concentrations of up to 10 $\mu$g/ml (Nimmanapalli *et al.,* 2002; Daniels *et al.,* 2004). Treatment with the ISS610 peptidomimetic, or the inactive, nonphosphorylated analog ISS610NP was at a final concentration of 1 mM for 24 h. All inhibitor stock solutions were prepared in dimethyl sulfoxide (DMSO) and subsequently were added to serum containing medium to obtain the final concentrations designated. For cell dissociation, cells were treated with EGTA/EDTA buffer (0.5 mM EGTA, 0.5 mM EDTA in phosphate-buffered saline; Rothen-Rutishauser *et al.,* 2002) for 60 min and extracted immediately for Stat3-ptyr705 determination. In all cases, cell viability was assessed by trypan blue exclusion and by replating in medium lacking the inhibitors.

Cell confluence was estimated visually and carefully quantitated by imaging analysis of live cells under phase contrast as well as fixed cells stained with Coomassie blue, using a Leitz Diaplan microscope (Rockleigh, NJ) and the MCID-elite software (Imaging Research, St. Catharines, Ontario, Canada). Both techniques gave very similar results, and numbers shown are averages of at least three independent experiments (Vultur *et al.,* 2004).

For all gene expression experiments involving examination of Stat3 activity assays, we used lines stably expressing these constructs, because we have previously found that transfection procedures can transiently activate Stat3, possibly because of a disturbance in cell to cell adhesion due to the presence of the precipitate (Arulanandam *et al.,* 2005). TAg expression was achieved through a pBabe-hygro based retroviral vector system as described (Raptis *et al.,* 1997a). The K1 mutant, which is defective in pRb binding, was expressed with a pBabe-puro retroviral vector (a gift of Dr. Thomas Roberts and Ole Gjoerup). In each case, 10T½, NIH3T3 or F111 fibroblasts were infected and selected for hygromycin resistance, and a number of independent clones were picked and tested for TAg levels. Representative clones, expressing different TAg levels, were chosen for further study. The Cre recombinase was expressed through infection with a pBabe-puro based retroviral vector. Cre expressing lines were recloned several times to ensure that all nonexpressing cells were eliminated. Stat3 was expressed through plasmid transfection under control of the CMV promoter (Turkson *et al.,* 1998) and Stat3C through retroviral vector infection (McLemore *et al.,* 2001).

The Jak2−/− cells were a generous gift of Dr. Ihle and Dr. Parganas of St. Jude's Hospital, Memphis, TN. The Src dominant-negative mutant was a gift of Dr. Elliott. It was prepared by cloning the K295R/Y527F mutant of chicken c-src into the *Eco*RI site of the pBabe–puro plasmid and the mutant expressed through infection of culture supernatant of the psi-2 packaging cells transfected with this construct, as previously described (Hung and Elliott, 2001). The adenovirus vector expressing the C-terminal Src kinase (Ad-Csk) was a generous gift of Dr. D. R. Kaplan. Ad-Csk was prepared by cloning the Csk gene in the GFP-expressing shuttle vector pAdTrack, recombined with the adenoviral vector pAdEasy by coelectroporation in bacteria, linearized, transfected, and amplified in 293 cells according to the manufacturer's instructions (Stratagene, La Jolla, CA; He *et al.,* 1998). This vector also expresses a green fluorescence protein (GFP) from a separate cytomegalovirus (CMV) promoter, which allows for easy identification of infected cells. High titer virus stocks were produced and the virus purified by CsCl centrifugation and titrated on 293 cells. 10T½ or 10T½-TAg-1 cells were infected with the Ad-Csk vector or the control pAdTrack lacking an insert at 50 pfu/ml and lysed 48 h later. In both cases, infection rates were more than 90%, as determined by fluorescence microscopy of the GFP protein, which is expressed from a separate CMV promoter (Angers-Loustau *et al.,* 2004). The same adenovirus vector was used to express the SrcDN mutant as before (Angers-Loustau *et al.,* 2004).

To examine the cells' ability for anchorage-independent proliferation, ~$10^4$ cells were suspended in 2 ml of 0.33% Agarose (Sigma, St. Louis, MO) containing Dulbecco's modified Eagle's medium supplemented with 15% FCS, on top of a feeder layer of the same medium containing 0.7% agarose, in 6-cm petri dishes (Raptis *et al.,* 1997a). Growth was recorded and photographs were taken 20 d later under brightfield illumination. Quantitation was achieved by suspending the cells in 2 ml of methocel (Sigma) containing 10 $\mu$Ci [$^3$H]thymidine per ml. Twenty days later, cells were washed from the water-soluble methocel, and trichloroacetic acid–precipitable counts were determined (Grammatikakis *et al.,* 2002).

### *Western Blotting and In Vitro Kinase Assays*

Cells were grown to different densities and proteins extracted using 50 mM HEPES, pH 7.4, 150 mM NaCl, 10 mM EDTA, 10 mM $Na_4P_2O_7$, 100 mM NaF, 2 mM $Na_3VO_4$, 0.5 mM phenylmethylsulfonyl fluoride, 10 $\mu$g/ml aprotinin, 10 $\mu$g/ml leupeptin, and 1% Triton X-100 (Raptis *et al.,* 2000). Fifty micrograms of clarified cell extract was resolved on a 10% polyacrylamide-SDS gel and transferred to a nitrocellulose membrane (Bio-Rad, Hercules, CA). The membranes were blocked with 5% nonfat milk for at least 1 h, followed by an overnight incubation in primary antibody. To increase sensitivity when comparing Stat3-ptyr705 levels between different lines, cells were sparsely grown to 15−25% confluence, while 100 $\mu$g protein loaded onto the gel and blots were exposed for longer times.

Immunodetection was performed using antibodies against the tyrosine-705 phosphorylated, i.e., activated form of Stat3 (BioSource International, Camarillo, CA), or against total Stat3 (Cell Signaling, Beverly, MA, Cat. no. 9132), followed by alkaline phosphatase–conjugated goat secondary antibodies (Biosource, Cat. no. ALI 4405). The bands were visualized using enhanced chemiluminescence (ECL), according to the manufacturer's instructions (PerkinElmer Life Sciences, Boston, MA, Cat. no. NEL602). To examine TAg levels, we used the antibody pAB108 (PharMingen, San Diego, CA). For FAK ptyr861 levels, blots were probed with a polyclonal antibody (Biosource International, Cat. no. 44-626G). For Jak1 and Jak2 in vitro kinase assays, extracts were precipitated with the HR785 antibody to Jak1 (Santa Cruz Biotechnology, Santa Cruz, CA, Cat. no. sc-277) or Jak2 (Biosource International, Cat. no. 44-406G), and 50 $\mu$l packed Staph. A-Sepharose beads (Pharmacia). [$\gamma$-$^{32}$P]ATP, 50 $\mu$Ci, was added to washed immunoprecipitates, eluted proteins resolved by PAGE, and autoradiography as previously described (Zhang *et al.,* 2000). Alternatively, Jak1 or Jak2 immunoprecipitates were blotted with the py99 anti-phosphotyrosine antibody (Santa Cruz, Cat. no. sc-7020). Jak3 kinase activity was assessed as above by immunoprecipitation with the AI-14-16 antibody (Labvision, Fremont, CA; Johnston *et al.,* 1994; Witthuhn *et al.,* 1994). c-Abl activity was measured by probing c-Abl immunoprecipitates (Santa Cruz Biotechnology, Cat. no. sc131, K12) with the anti-phosphotyrosine antibody py99 as previously described (Huang *et al.,* 2002). In all cases, as a control for protein loading parallel blots were routinely probed with the mouse monoclonal anti-Hsp90 antibody (Stressgen Biotechnologies, Victoria, British Columbia, Canada, Cat. no. SPA-830), followed by a secondary antibody and ECL detection as above. Quantitation was achieved by phosphorimager analysis using a Molecular Dynamics Storm PhosphorImager (Sunnyvale, CA) and the ImageQuant program, or by fluorimager analysis using the FluorChem program (Alpha Innotech, San Leandro, CA), with the values obtained normalized for Hsp90.

### *Electrophoretic Mobility Shift Assays*

The procedures for nuclear extract preparation from NIH3T3 fibroblasts or their v-Src–transformed counterparts and electrophoretic mobility shift assays (EMSAs) were essentially as previously described (Yu *et al.,* 1995). The $^{32}$P-labeled oligonucleotide probe used was the hSIE (high-affinity *sis*-inducible element, m67 variant, 5′-AGCTTCATTTCCCGTAAATCCCTA) that binds both Stat1 and Stat3 (Wagner *et al.,* 1990). For supershift assays, 1 $\mu$g of the anti-Stat3 antibody was preincubated with the nuclear cell extract for 30 min before the addition of the radiolabeled probe (Zhang *et al.,* 2000). The reactions were incubated at 30°C for 30 min and then resolved on nondenaturing, 5% polyacrylamide gels in Tris-Borate-EDTA buffer. Stat3-DNA com-

plexes were detected by autoradiography. Quantitation was achieved by phosphorimager analysis.

### *Luciferase Assays for Stat3 Transcriptional Activity*

NIH3T3 cells were transfected with a Stat3-specific reporter plasmid (p*Luc*TKS3) which harbors seven copies of a sequence corresponding to the Stat3-specific binding site in the C-reactive gene promoter (termed APRE, TTCCCGAA) upstream from a firefly luciferase coding sequence (Turkson *et al.,* 1998), with puromycin-resistance coselection. Individual clones were grown up and screened for firefly Luciferase activity, measured in total cell extracts according to the manufacturer's protocol (Promega, Madison, WI, Cat. no. E4030). As a control, p*Luc*TKS3-expressing cells were stably transfected with a different reporter, pRLSRE, which contains two copies of the serum response element (SRE) of the c-fos promoter, subcloned into the *Renilla* luciferase reporter, pRL-null (Promega), and Zeocin (Invitrogen, Burlington, Ontario, Canada)-resistance coselection (Turkson *et al.,* 2001). The firefly and *Renilla* luciferases utilize different substrates and thus can be assayed independently in the same lysates using this kit. TAg was subsequently introduced in NIH3T3 cells expressing both reporters through infection with the retroviral vector above, and luciferase activities measured at different densities.

### *siRNA Expression*

A Stat3-specific siRNA oligonucleotide, AATTAAAAAAGTCAGGTTGCTGGTCAAATTCTCTTGAAATTTGACCAGCAACCTGACTTCC was inserted into the pSilencer 1.0-U6 siRNA expression vector (Ambion, Austin, TX, Cat. no. 5760-5766) and cotransfected with pBabe-puro DNA into TAg-expressing, 10T½ cells (clone 10T½-TAg-1), followed by puromycin resistance selection. Clones stably transfected with the empty pSilencer 1.0-U6 vector and pBabe-puro were used as controls. To ensure siRNA function, cell extracts were probed for total Stat3 in Western blots. Cells were recloned several times to ensure siRNA expression was stable and all nonexpressing cells were eliminated.

## RESULTS

### *Simian Virus 40 Large Tumor Antigen Stimulates Stat3 Activity*

To examine the effect of tumor antigen (TAg) on Stat3 activity, this oncogene was expressed in mouse NIH3T3, 10T½, or rat F111 fibroblasts through infection with the culture supernatant from a packaging line expressing a pBabe-hygro–based retroviral vector coding for TAg (Raptis *et al.,* 1997a). As a control, a vector lacking the TAg insert was used to infect the same target lines. After selection in hygromycin-containing medium for 2–3 wk, individual colonies were picked, expanded into clones, and screened for levels of TAg expression by Western blotting. Clones expressing different amounts of TAg were chosen for further analysis of Stat3 activity levels (see *Materials and Methods* and Figure 1).

Previous results revealed a dramatic increase in Stat3 activity with cell density, which gradually declined at later stages (Vultur *et al.,* 2004). Therefore, to examine the effect of TAg per se on Stat3 activity, Stat3 tyr-705 phosphorylation was assessed at different levels of confluence in 12 representative clones expressing progressively increasing amounts of TAg (e.g., line 10T½-TAg-1, Figure 1A and Table 1). As a control for protein loading, the same extracts were probed for the abundant heat-shock protein, Hsp90 (Figure 1E). As observed before (Vultur *et al.,* 2004), Stat3-ptyr705 levels were very low in the parental 10T½ cells, when grown to confluences of 60% (lane 1) or less, but dramatically increased with cell density, with a peak at 1–2 d postconfluence (lane 4). As shown in Figure 1A, however (lanes 6–10), TAg-expressing cells displayed substantially higher Stat3–705 phosphorylation levels than the parental line at all densities, whereas a careful quantitation revealed that the relative increase on TAg expression was the same regardless of cell confluence. This increase was proportional to the levels of TAg present (Table 1), whereas cells with the highest TAg expression (e.g., 10T½-TAg-1) displayed Stat3 levels comparable to the levels in cells expressing the known Stat3 activator, v-Src (lane 12). In addition, phosphorylation of Stat3-ser727 increased as well with TAg expression, although to a slightly lesser extent than Stat3-ptyr705 (Figure 1C). To ensure that cell density did not affect TAg expression itself, TAg levels were also examined at all densities and found to be unchanged (Figure 1D). Cell lines with lower TAg levels (e.g., 10T½-TAg-2, 10T½-TAg-3), had proportionately lower Stat3 ptyr-705 levels (Table 1). Similar results were obtained with mouse NIH 3T3 and rat F111 fibroblasts after transformation by TAg. In addition, growth of the human AR5 line harboring a temperature-sensitive TAg mutant (Radna *et al.,* 1989) at the permissive temperature of 33°C resulted in a significant increase in Stat3 ptyr-705 levels, compared with cells grown at 39°C (unpublished data). The above data taken together indicate that TAg expression results in stimulation of Stat3–705 phosphorylation at all levels of density of cultured fibroblasts.

The levels of total Stat3 protein were examined next. As previously reported (Vultur *et al.,* 2004), total Stat3 protein levels increased with cell density in all lines tested (Figure 1B), possibly because of the ability of Stat3 to activate its own promoter (Narimatsu *et al.,* 2001), although the differences were not as pronounced as the Stat3–705 phosphorylation (Figure 1A). Total Stat3 levels were higher in TAg-expressing cells, indicating that TAg expression can trigger an increase in total Stat3 protein as well, possibly through Stat3 activation of its own promoter.

Previous results indicated that disruption of cell to cell adhesion at postconfluence through Calcium chelation abrogated Stat3 activation (Vultur *et al.,* 2004). To ensure that TAg can activate Stat3, independently from the expected activation induced by cell to cell contact increases because of changes in cell morphology brought about by transformation, cell contacts were disrupted in cells grown to different densities through Calcium chelation by EGTA/EDTA treatment (see *Materials and Methods*). As shown in Figure 1F (top panel), calcium chelation caused a dramatic reduction in Stat3-ptyr705, at all densities of both normal and TAg-expressing cells. However, TAg-transformed cells displayed a substantial amount of residual Stat3 tyrosine phosphorylation. Together with the fact that TAg-expressing cells had higher Stat3-ptyr705 levels than normal ones even when sparsely grown, these results suggest that TAg can activate Stat3 independent from cell-cell adhesion (compare Figure 1, A and F). To further examine the specificity of the TAg-mediated, Stat3 activation, Stat3-ptyr705 levels were examined in 10T½ cells stably expressing activated $Ras^{leu61}$ (Raptis *et al.,* 1997b). As shown in Figure 1G, $Ras^{leu61}$ expressing, 10T½ cells (Raptis *et al.,* 1997b) had the same Stat3-ptyr705 levels as the parental 10T½, indicating that Stat3 tyrosine phosphorylation is not simply a general outcome of the transformed state.

To examine whether this increase in phosphorylation by TAg is accompanied by an increase in Stat3 DNA-binding competence, we performed Stat3 DNA-binding studies using the hSIE probe, which specifically binds Stat1 and Stat3. After labeling, this probe was added to nuclear extracts from 10T½ or 10T½-TAg-1 cells, in EMSA (see *Materials and Methods*). As shown in Figure 1H, the amount of Stat3 bound to the hSIE probe paralleled the increase in Stat3-ptyr705 phosphorylation. Supershift analysis using antibodies to total Stat3 indicated that the bands obtained consist of complexes of Stat3 specifically(lanes 1 and 10; Wagner *et al.,* 1990). We further examined the effect of TAg on Stat3 transcriptional activity, by introducing TAg in NIH3T3 cells stably express-

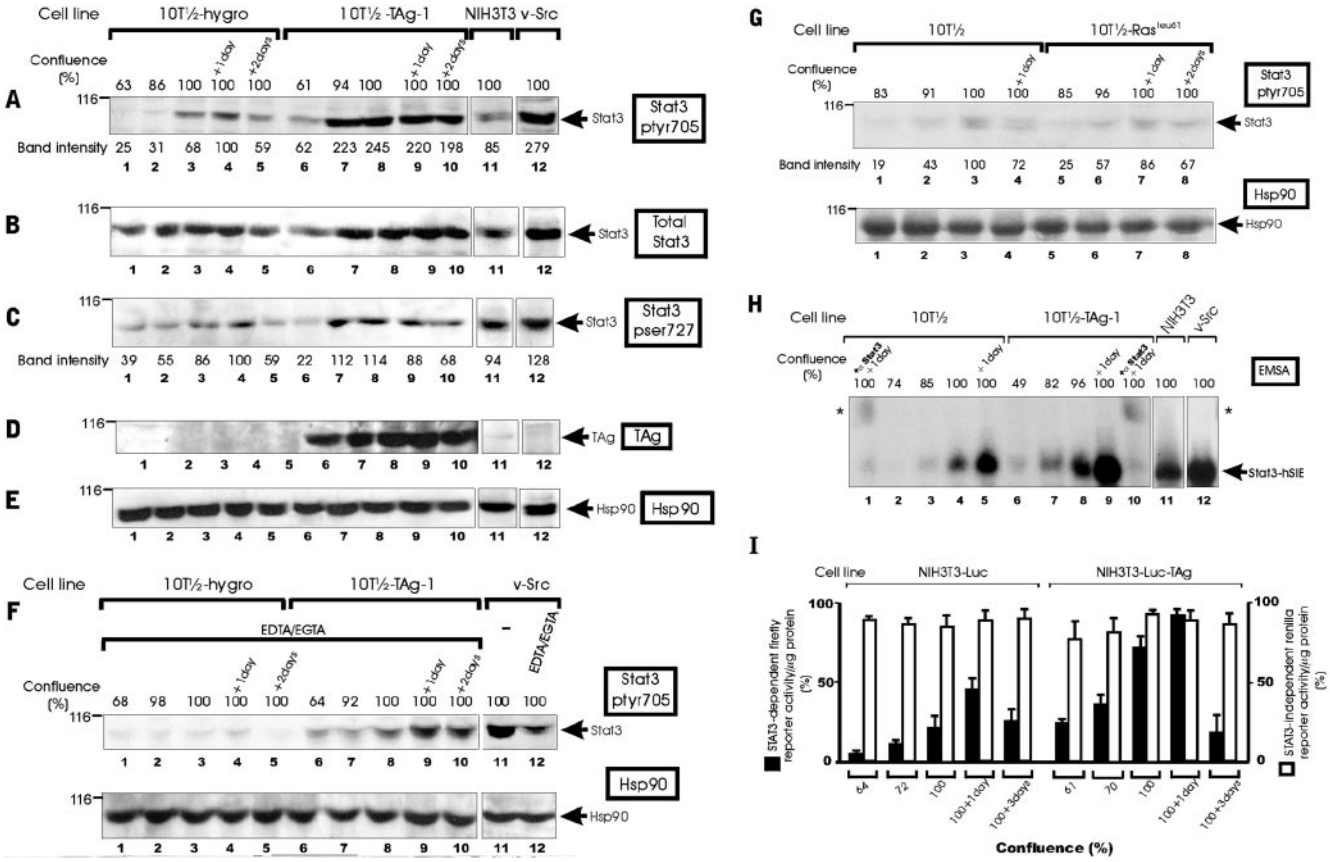


**Figure 1.** TAg up-regulates Stat3 activity at all levels of confluence. Lysates from normal mouse 10T½ fibroblasts, before (lanes 1–5), or after (lanes 6–10) TAg expression (line 10T½-TAg-1, Table 1), grown to different degrees of confluence and up to 2 d postconfluence as indicated, were resolved by gel electrophoresis. Western immunoblots were probed for A, the tyr705-phosphorylated form of Stat3; B, total Stat3 protein; C, Stat3-pser727, D, TAg; E, Hsp90 as a loading control, as indicated. Lanes 11 and 12: NIH 3T3 cells, before and after transformation by v-Src, as indicated. Fifty micrograms of lysate was loaded in all cases. Numbers at the left refer to molecular-weight markers. Arrow points to the position of Stat3-ptyr705, total Stat3, TAg, or Hsp90, respectively. Numbers under lanes in A and C refer to band intensities obtained through quantitation by fluorimager analysis, with the peak value of the control 10T½-hygro cells taken as 100% (see *Materials and Methods*). (F) TAg activates Stat3 even in the absence of cell-to-cell adhesion. 10T½ (lanes 1–5) or TAg-transformed, 10T½-TAg-1 (lanes 6–10) cells were grown to different densities and then detached from the petris by EGTA/EDTA treatment for 1 h and vigorous pipetting (see *Materials and Methods*). Lanes 11 and 12: vSrc-transformed, NIH3T3 cells, before (lane 11) or after (lane 12) EGTA/EDTA treatment, as indicated. Cell lysates were probed for Stat3-ptyr705 (top panel) or Hsp90 (bottom panel) as above. (G) Ras$^{leu61}$ does not induce Stat3-ptyr705 phosphorylation. Lysates from 10T½ fibroblasts before (lanes 1–4) or after (lanes 5–8) Ras$^{leu61}$ expression (Raptis *et al.*, 1997b) grown to different densities were blotted and probed for Stat3-ptyr705 as above. Numbers under the lanes refer to band intensities obtained through quantitation by fluorimager analysis, with the peak value of the parental 10T½ cells taken as 100% (see *Materials and Methods*). (H) Autoradiogram of Stat3-hSIE complexes in nuclear extracts from 10T½ (lanes 1–5) or 10T½-TAg-1 (lanes 6–10) cells prepared at the indicated cell densities. Arrow points to the position of the complex Stat3:hSIE. In lanes 1 and 10, the same extracts as in lanes 5 and 9, respectively, were incubated with anti-Stat3 antibodies. Lanes 11 and 12: NIH 3T3 cells, before and after transformation by v-Src, as indicated. The position of the supershifted Stat3-hSIE-antibody complex is indicated with an asterisk. (I) TAg activates Stat3 transcription. TAg was expressed in NIH3T3 cells stably expressing the Stat3-dependent p*Luc*TKS3 reporter driving a firefly luciferase gene under control of the hSIE promoter element, and the Stat3-independent pRLSRE reporter driving a *Renilla* luciferase gene under control of the c-fos SRE promoter, respectively (NIH3T3-Luc cells). Control and TAg-expressing cells were grown to the indicated densities with daily media changes and firefly (■) and Renilla (□) luciferase activities determined in cytosolic extracts (see *Materials and Methods*). Values shown represent luciferase units expressed as a percentage (%) of the highest value obtained, means plus SD of at least three experiments, each performed in triplicate.

ing a firefly Luciferase gene construct under control of a Stat3-specific promoter (p*Luc*TKS3 plasmid) and a Renilla Luciferase gene under control of a Stat3-independent, c-fos, SRE promoter (see *Materials and Methods*; Vultur *et al.*, 2004). As shown in Figure 1I, there was a dramatic increase in Stat3-dependent transcription upon TAg expression at all densities examined, whereas no effect was observed upon the transcription from the Stat3-independent c-fos, SRE promoter, indicating that TAg induces a Stat3 activity increase specifically. The above data taken together indicate that TAg expression is the trigger for a further increase in Stat3 tyrosine phosphorylation, DNA binding, and transcriptional activity specifically, at all levels of confluence.

### *TAg Requires Stat3 Activity In Order To Induce Neoplastic Transformation*

To examine the role of Stat3 upon TAg-induced neoplasia, the ability of TAg to transform cells in the face of low Stat3 activity levels was examined using lines that were rendered deficient in Stat3 activity. Two different approaches for Stat3 down-regulation were used: 1), a conditional Stat3-knockout using a cre-loxP system, and 2), a Stat3-specific siRNA.

**Table 1.** Rb inactivation activates Stat3, which is required for neoplastic transformation

| Cell line[a] | Stat3-705 (%)[b] | TAg (%)[c] | Transformation | | |
|---|---|---|---|---|---|
| | | | Methocel (%)[d] | Foci (%)[e] | Growth rate (h)[f] |
| 10T½ | 100 ± 15 | — | 0 | 0 | 24 |
| 10T½-hygro[g] | 100 ± 16 | — | 0 | 0 | 24 |
| 10T½-TAg-1 | 255 ± 18 | 100 | 100 | 100 | 19 |
| 10T½-TAg-2 | 212 ± 17 | 85 | 55 | 92 | 20 |
| 10T½-TAg-3 | 144 ± 16 | 32 | 20 | 63 | 22 |
| Stat3-loxP–expressing cells | | | | | |
| flox[h] | (100) ± 15 | — | 0 | 0 | 23 |
| flox-puro[h] | (100) ± 16 | — | 0 | 0 | 23 |
| flox-SV-1 | (253) ± 22 | 100 | 100 | 100 | 19 |
| flox-Cre[i] | (11) ± 3 | − | 0 | 0 | 42 |
| flox-SV-Cre-1 | (27) ± 3 | 100 | 0 | 0 | 39 |
| flox-SV-Cre-1-Stat3[l] | (210) ± 30 | 100 | 85 | 95 | 22 |
| flox-SV-Cre-1-Stat3C[m] | (250) ± 21 | 100 | 115 | 110 | 22 |
| SV-flox-1[n] | (220) ± 19 | 100 | 100 | 100 | 19 |
| SV-flox-1-Cre-1 | (13) ± 4 | 100 | 0 | 0 | 43 |
| siRNA-expressing clones | | | | | |
| 10T½-TAg-1-U6 | 257 ± 10 | 100 | 100 | 100 | 19 |
| 10T½-TAg-1-si | 12 ± 3 | 100 | 10 | 23 | 49 |
| 10T½-si | 15 ± 2 | — | 0 | 0 | 60 |
| 10T½-TAg-1-si-Stat3[l] | 230 ± 25 | 100 | 90 | 88 | 24 |
| E1A-expressing clones | | | | | |
| 10T½ | 100 ± 17 | — | 0 | 0 | 24 |
| 10T½-E1A-1[o] | 251 ± 18 | — | 40 | 100 | 20 |
| 10T½-E1A-2 | 198 ± 13 | — | 20 | 82 | 20 |
| 10T½-E1A-3 | 184 ± 16 | — | 10 | 51 | 20 |
| Cells defective in pRb family members | | | | | |
| pRb−/− | 265 ± 23 | — | 10 | 58 | 20 |
| p130−/− | 100 ± 15 | — | 0 | 0 | 24 |
| TKO[p] | 240 ± 20 | — | 95 | 100 | 19 |
| wt 3T3 | 100 ± 16 | — | 0 | 0 | 21 |

[a] For illustration purposes, only some of the clones are presented.

[b] Lysates from the indicated lines were resolved by gel electrophoresis, and Western immunoblots were probed for the tyr705-phosphorylated form of Stat3. Numbers represent relative values obtained by quantitation analysis. Averages ± SEM of at least three experiments are shown, with the average of the value for NIH3T3 or 10T½ cells taken as 100% (see *Materials and Methods*). In all cases, the EMSA values obtained paralleled the Stat3–705 phosphorylation levels. Data from sparsely growing cells are presented, but the relative increases did not change significantly with cell density.

[c] TAg levels were determined by Western blotting (see *Materials and Methods*).

[d] Approximately 200 cells were seeded together with 10,000 normal cells in 6-cm plates. Cells were stained with Coomassie blue, and foci were scored 10 days later.

[e] Anchorage-independent growth was quantitated by suspending 50,000 cells in 2 ml Methocel containing 10 $\mu$Ci/ml [$^3$H]thymidine and measuring incorporation 20 d later (see *Materials and Methods*). Numbers represent percentages, with the levels of the highest expresser, 10T½-TAg-1, defined as 100%.

[f] 30,000 cells were seeded in 60-mm dishes and counted at several time points over 7 d. Doubling times are shown in hours.

[g] 10T½ cells infected with the pBabe-hygro retroviral vector lacking an insert (Raptis *et al.*, 1997a).

[h] Cells spontaneously established from Stat3-flox mouse embryos. The values for Stat3-705 are in parentheses to indicate the presence of the loxP sequences. flox-puro refers to flox cells infected with the pBabe-puro retroviral vector and selected for puromycin resistance.

[i] Cells expressing the Cre recombinase through retroviral vector infection.

[l] Stat3 was reintroduced in flox-SV-1-Cre cells (see *Materials and Methods*).

[m] The constitutively active, Stat3C mutant was introduced into flox-SV-1-Cre cells (see *Materials and Methods*).

[n] Cells from Stat3-flox mouse embryos, established through TAg expression.

[o] 10T½ cells expressing E1A through retroviral vector infection. 10T½-E1A-1, 10T½-E1A-2, and 10T½-E1A-3 express 80, 60, and 30%, respectively, the E1A levels of the prototype, 293 line (Cao *et al.*, unpublished results).

[p] Triple knockouts, i.e., fibroblasts from mice where pRb, p107, and p130 have been deleted.

### *Cre-loxP*

To examine the Stat3 requirement for TAg-mediated transformation, we made use of the Cre-loxP recombination system, to introduce a genetic ablation of the Stat3 gene (Akira, 2000). Primary fibroblasts were prepared from mouse embryos in which two loxP sites had been introduced 5′ and 3′ of the exon encoding the tyrosine-705 residue critical for Stat3 activation (Akira, 2000). After spontaneous establishment of these cells in culture, TAg was expressed using the same retroviral vector as above. Five lines, expressing high TAg levels (e.g., line flox-SV-1, Table 1) were chosen for further analysis. Parallel cultures were immortalized through TAg expression directly and selected for hygromycin resistance, and six lines, expressing TAg levels similar to

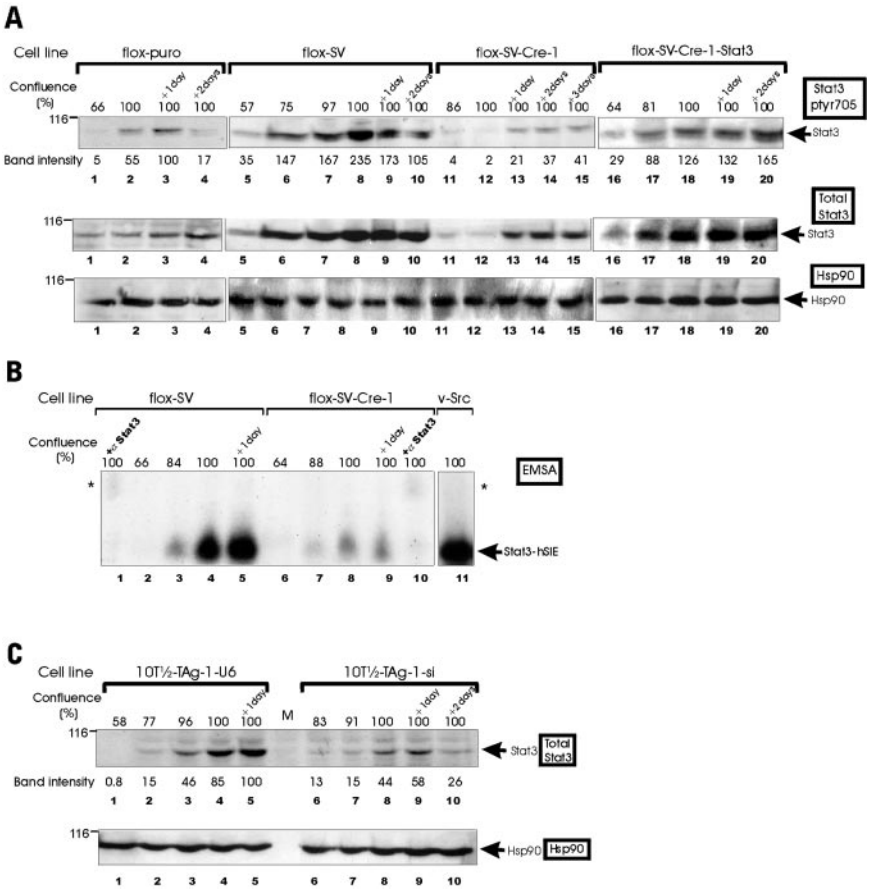


**Figure 2.** TAg expression in Stat3-deficient lines. Stat3 down-regulation using the Cre-loxP system. Lysates from spontaneously established, pBabe-puro–infected, flox-puro (lanes 1–4) or flox-SV (lanes 5–10) cells, before (lanes 1–10) or after (lanes 11–20) expression of the Cre recombinase, grown to different degrees of confluence and up to 3 d postconfluence as indicated, were resolved by gel electrophoresis. Lanes 16–20: add-back experiments where the Stat3 gene was reintroduced in flox-SV-Cre-1 cells through transfection (see *Materials and Methods*). Western immunoblots were probed for (top panel) the tyr705 phosphorylated form of Stat3; (middle panel) total Stat3 protein; and (bottom panel) Hsp90. Fifty micrograms of lysate was loaded in all cases. Numbers at the left refer to molecular-weight markers. Arrow points to the position of Stat3-ptyr705, total Stat3, or Hsp90, respectively. Numbers under the lanes refer to band intensities obtained through quantitation by fluorimager analysis, with the peak value of the control flox-puro cells taken as 100% (see *Materials and Methods*). (B) Autoradiogram of Stat3-hSIE complexes in nuclear extracts from flox-SV-1 or flox-SV-Cre-1 cells prepared at the indicated densities. Arrow points to the position of the complex Stat3:hSIE. In lanes 1 and 10, the same samples as in lanes 5 and 9 were incubated with anti-Stat3 antibodies. The position of the supershifted Stat3-hSIE-antibody complex is indicated with an asterisk. (C) Stat3 down-regulation through stable Stat3-siRNA expression: TAg expressing, 10T½-TAg-1 cells were transfected with a plasmid coding for a Stat3-specific, siRNA (lanes 6–10) or the control plasmid (lanes 1–5) and grown to different densities as above. Lysates were probed for total Stat3 (top panel) or Hsp90 (bottom panel). (M) Molecular-weight marker lane. Numbers under the lanes refer to band intensities obtained through quantitation by fluorimager analysis, with the peak value of the control 10T½-TAg-1-U6 cells taken as 100% (see *Materials and Methods*).

10T½-TAg-1, were used in further experiments (e.g., line SV-flox-1, Table 1). To inactivate Stat3 function, flox cells were infected with a pBabe-puro–based, retroviral vector carrying the Cre recombinase, selected for puromycin resistance and individual colonies examined. As shown in Figure 2A, Cre expression caused a dramatic reduction in both total and tyrosine-phosphorylated Stat3 at all densities examined, compared with control cells infected with a vector lacking a Cre insert (flox-puro), as demonstrated by Western blotting using antibodies against total Stat3 or Stat3-ptyr705 (Figure 2A, lanes 5–10 vs. 11–15, and Table 1), or EMSA assays (Figure 2B).

Examination of the cellular phenotype revealed that Stat3 down-regulation through Cre infection dramatically reduced the rate of cell proliferation. The doubling time of the spontaneously established, flox cells was 23 h, and it increased to 42 h after Cre expression, whereas TAg expression did not overcome this defect (Table 1). In addition, growth in agar and formation of foci overgrowing a monolayer of spontaneously established, flox cells were dramatically reduced after Cre infection, compared with the parental flox-SV (Figure 3, A and B, and Table 1). In fact, Cre expressing, flox-SV-Cre-1 cells entered apoptosis upon formation of extensive cell-to-cell contacts (see below). At the same time, reintroduction of Stat3 in flox-SV-Cre-1 cells through transfection (Turkson *et al.*, 1998; see *Materials and Methods*; Figure 2A, lanes 16–20), restored the cells' growth rate, focus-forming ability, and anchorage-independence (Table 1). These data indicate that genetic ablation of the Stat3 exon encoding tyr705 inhibits transformation by TAg.

### *siRNA*

A Stat3-specific siRNA oligonucleotide was inserted into the pSilencer 1.0-U6 siRNA expression vector (see *Materials and Methods*) and cotransfected with a pBabe-puro plasmid into TAg-expressing, 10T½ cells (clone 10T½-TAg-1), followed by puromycin resistance selection. A large number of individual clones were picked and screened for total Stat3 by Western blotting, and clones with low Stat3 levels (e.g., 10T½-TAg-1-si) were chosen for further experimentation. Clones stably transfected with the empty pSilencer 1.0-U6 vector and pBabe-puro were used as controls (e.g., 10T½-TAg-1-U6). As shown in Figure 2C and Table 1, siRNA expression had a dramatic effect on Stat3 levels; transfected cells displayed ~12–15% the total Stat3 levels present in control cells. Examination of the cellular phenotype showed that, same as in the flox-SV-Cre-1 cells expressing the Cre recombinase, the ability of clones expressing the Stat3-specific, siRNA to grow in an anchorage-independent manner or to form foci overgrowing a monolayer of normal 10T½ cells was dramatically reduced compared with the parental 10T½-TAg-1 or the control 10T½-TAg-1-U6 (Table 1). In addition, siRNA expression in TAg-transformed rat F111 cells caused a dramatic reversal of the cells' transformed

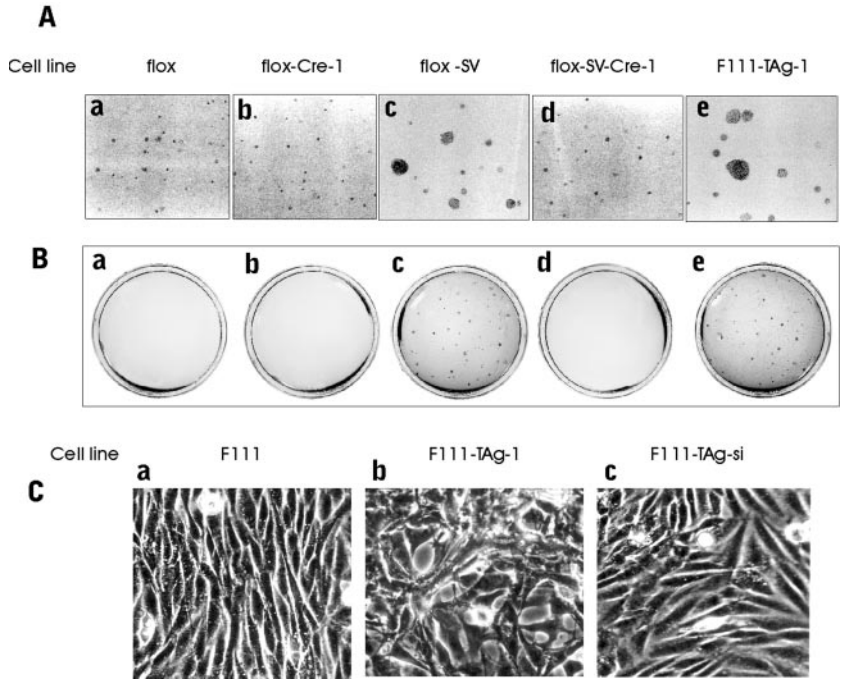


**Figure 3.** Stat3 deficiency prevents TAg-mediated transformation. (A) Anchorage-independent growth: flox (a), flox-Cre-1 (b), flox-SV (c), flox-SV-Cre-1 (d), or TAg-transformed rat F111, F111-TAg (Raptis *et al.*, 1997a; e) cells were suspended in soft agarose. Twenty days later cells were photographed under brightfield illumination. Magnification, 40×. (B) Formation of foci: 200 flox (a), flox-Cre-1 (b), flox-SV (c), flox-SV-Cre-1 (d), or F111-TAg (e) cells were plated in 60-mm Petri dishes together with 10,000 normal flox cells. Petris were fixed, stained with Coomassie blue, and photographed 10 d later. (C) Morphology on plastic: normal rat F111 fibroblasts before (a) or after transformation by TAg (b, line F111-TAg-1) or F111-TAg cells expressing the Stat3-specific, siRNA (c) were photographed under phase-contrast illumination. Magnification, 240×.

morphology on plastic (Figure 3C), a characteristic previously shown to be very sensitive to low levels of expression of oncogenes such as TAg or the middle tumor antigen of polyoma virus (Raptis *et al.*, 1985; Grammatikakis *et al.*, 2001).

To ensure that the inhibition of transformation was indeed due to Stat3 down-regulation, Stat3 activity levels were restored to normal through transfection with a construct coding for Stat3 as above, which returned the Stat3 levels of the 10T½-TAg-1-si cells to nearly the levels in the parental 10T½-TAg-1 (Table 1). Add-back expression of Stat3 increased the rate of cell growth and restored the cells' ability for anchorage-independent proliferation (Table 1). As a control, expression of the Stat3 gene alone did not result in transformation of 10T½ cells, indicating that it is the restoration of Stat3 levels to normal in siRNA-expressing cells that is responsible for restoration of the cells' transformation phenotype. In addition, expression of the constitutively active form of Stat3, Stat3C (Bromberg *et al.*, 1999) through infection with a retroviral vector (McLemore *et al.*, 2001) had a similar effect (Table 1).

The above data taken together indicate that TAg requires the activity of Stat3 to induce neoplastic transformation of cultured rodent fibroblasts.

### *pRb Binding Is Required for the TAg-mediated Stat3 Activation*

One of the cellular targets of TAg is the retinoblastoma-susceptibility gene product family (pRb, p107, p130). These proteins bind a group of transcription factors collectively termed E2F (E2F1 to E2F6), which are responsible for transcription of a number of genes involved in DNA replication and cell-cycle progression. pRb binds to and sequesters E2F and at the same time pRb actively suppresses transcription from E2F-responsive promoters (Trimarchi and Lees, 2002). TAg binds pRb family proteins at a specific sequence (LXCXE) and this association is sufficient to liberate E2Fs from their binding to pRb family members in rodent cells (Sullivan and Pipas, 2002). This results in up-regulation of E2F transactivation activity and subsequent progression into S phase (Zalvide *et al.*, 1998). We investigated the importance of pRb binding to and inactivation by TAg by expressing the nontransforming TAg mutant K1 (Glu107 to Lys), which is unable to bind pRb family proteins, in 10T½ cells to similar levels as the wild-type TAg in line 10T½-TAg-1 (see *Materials and Methods*). Stat3 phosphorylation was subsequently measured and compared with 10T½ cells at different levels of density. As shown in Figure 4A, Stat3 ptyr-705 levels in K1-expressing, 10T½ cells were similar to the parental line (lanes 1–5 vs. 6–10, respectively), indicating that Stat3 activation segregates with the ability of TAg to bind pRb and neoplastically transform rodent fibroblasts.

To further examine the effect of pRb inactivation on Stat3 phosphorylation, we assessed the effect of the adenovirus E1A gene product, known to bind to and inactivate pRb, upon Stat3 phosphorylation. The E1A, 243R (12S) gene was expressed in mouse 10T½ fibroblasts and three clones, with increasing levels of 243R protein, were chosen for further experiments. Cells were plated to different densities and Stat3-ptyr705 examined as above. As shown in Figure 4B, the introduction of E1A led to an increase in Stat3-ptyr705, in a manner proportional to E1A expression levels (Table 1), suggesting that pRb inactivation can lead to an increase in Stat3 activity.

To definitively demonstrate the role of pRb inactivation in Stat3 stimulation, we measured Stat3-ptyr705 levels in cells established from knockout mice where the pRb gene had been genetically ablated (pRb−/− cells; Sage *et al.*, 2000). pRb deletion in these cells liberates the activating E2F transcription factors and abrogates the G1 restriction point. As shown in Figure 4C, the pRb−/− cells had high Stat3-ptyr705 levels compared with their wild-type counterparts, at all densities examined (lanes 1–6 vs. 7–12). Similarly, genetic ablation of all three pRb family members (pRb, p107, and p130), in cells cultured from triple knockout (TKO) mice resulted in high Stat3 activity levels (lanes 13–17). On the other hand, cells established from p130−/− (Figure 4C, lanes 18–22) or p107−/− (unpublished data) mice did not display the same high Stat3-ptyr705 levels. As shown in

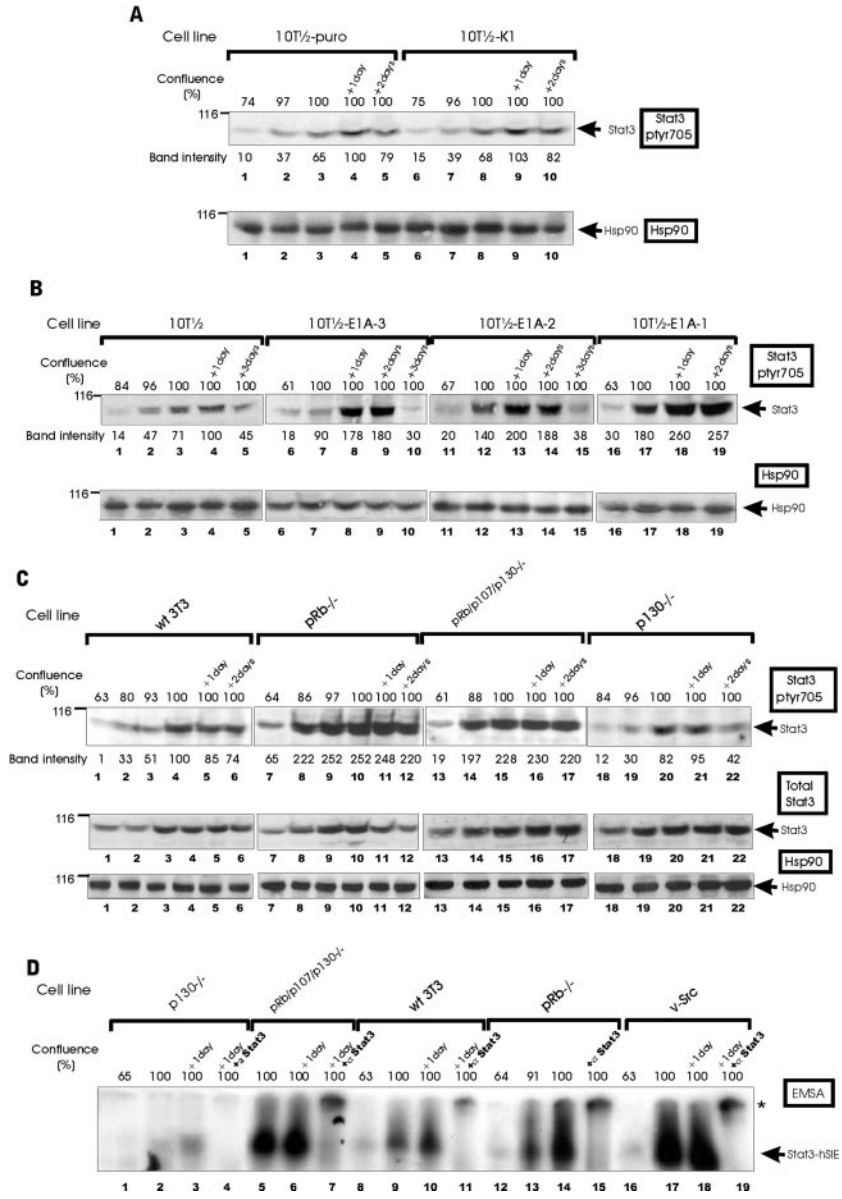


**Figure 4.** pRb inactivation leads to Stat3 tyrosine phosphorylation. (A) pRb binding by TAg is required for Stat3–705 phosphorylation. Lysates from control 10T½-puro cells (lanes 1–5) or 10T½ cells expressing the K1, TAg mutant that is defective in pRb binding (lanes 6–10), grown to different densities were resolved by gel electrophoresis. Western immunoblots were probed for (top panel) the tyr705-phosphorylated form of Stat3, and (bottom panel) Hsp90. Fifty micrograms of lysate was loaded in all cases. Numbers at the left refer to molecular-weight markers. Arrow points to the position of Stat3-ptyr705, as indicated. Numbers under the lanes refer to band intensities obtained through quantitation by fluorimager analysis, with the peak value of the control 10T½-puro cells taken as 100% (see *Materials and Methods*). (B) Expression of the adenovirus E1A, 243R protein increases Stat3 tyr705 phosphorylation. Extracts from 10T½ (lanes 1–5), 10T½-E1A-3 (lanes 6–10), 10T½-E1A-2 (lanes 11–15), and 10T½-E1A-1 (lanes 16–19) cells expressing increasing amounts of the E1A protein (Table 1), grown to different densities as indicated, were resolved by gel electrophoresis. Western immunoblots were probed for (top panel) the tyr705-phosphorylated form of Stat3, and (bottom panel) Hsp90. Fifty micrograms of lysate was loaded in all cases. Numbers at the left refer to molecular-weight markers. Arrow points to the position of Stat3-ptyr705, as indicated. Numbers under the lanes refer to band intensities obtained through quantitation by fluorimager analysis, with the peak value of the parental 10T½ taken as 100% (see *Materials and Methods*). (C) pRb ablation leads to Stat3 ptyr705 phosphorylation. Lysates from pRb−/− (lanes 7–12), p130−/− (lanes 18–22), pRb/p107/p130, triple knockout (lanes 13–17) cells, or their wild-type counterparts (lanes 1–6) grown to different densities were resolved by gel electrophoresis. Western immunoblots were probed for (top panel) the tyr705-phosphorylated form of Stat3; (middle panel) total Stat3; and (bottom panel) Hsp90, as indicated. Fifty micrograms of lysate was loaded in all cases. Numbers at the left refer to molecular-weight markers. Arrows point to the position of Stat3-ptyr705 or total Stat3, respectively, as indicated. Numbers under the lanes refer to band intensities obtained through quantitation by fluorimager analysis, with the peak value of the wild-type cells taken as 100% (see *Materials and Methods*). (D) EMSA assays. Autoradiogram of Stat3-hSIE complexes in nuclear extracts from pRb−/− (lanes 12–15), p130−/− (lanes 1–4), pRb/p107/p130, triple knockout (lanes 5–7) cells, or their wild-type counterparts (lanes 8–11), or control v-Src–expressing, NIH3T3 cells (lanes 16–19), prepared at the indicated cell densities. Arrow points to the position of the complex Stat3:hSIE. In lanes 4, 7, 11, 15, and 19, the same samples as in lanes 3, 6, 10, 14, and 18, respectively, were incubated with anti-Stat3 antibodies. The position of the supershifted Stat3-hSIE-antibody complex is indicated with an asterisk.

Figure 4D, EMSA assays showed a close correlation with the Stat3-ptyr705 phosphorylation levels. The above data taken together point to the possibility that inactivation of pRb by TAg may induce the observed Stat3-ptyr705 phosphorylation and activation.

### *Kinases Responsible for the TAg-induced Phosphorylation of Stat3*

STAT phosphorylation by cytokine receptors, which lack intrinsic tyrosine kinase activity, is mediated by the associated Janus kinases (JAKs). On the other hand, STAT phosphorylation and activation after stimulation of tyrosine-kinase receptors is a complex process; after ligand engagement, both Stat1 and Stat3 bind the phosphorylated EGF or PDGF receptors through their SH2 domains (Levy and Darnell, 2002). Although receptor tyrosine kinases would be able to directly phosphorylate Stat1 and Stat3, both the JAK and c-Src kinases are also required for PDGF- or EGF-induced STAT activation (Vignais *et al.*, 1996; Cirri *et al.*, 1997; Olayioye *et al.*, 1999; Vignais and Gilman, 1999; Wang *et al.*, 2000). To examine the involvement of Src family kinases in Stat3 phosphorylation after TAg expression, 10T½-TAg-1 cells were grown to different densities and treated with two Src-selective inhibitors, SU6656 and PD180970 (Zhang *et al.*, 2000; Garcia *et al.*, 2001) for 24 h, followed by examination of their Stat3-ptyr705 levels. The extent of Src inactivation was

monitored through examination of phosphorylation of the Src substrate, focal adhesion kinase (FAK) at tyr861, shown to be a major site of phosphorylation by c-Src (Calalb *et al.*, 1996), using an antibody specific for this site (Gabarra-Niecko *et al.*, 2003). As shown in Figure 5, A and B, both Src inhibitors caused a dramatic reduction in Stat3-ptyr705 in TAg-transformed cells (lanes 1–5 vs. 6–10). This inhibition was more pronounced in sparse cells, whereas when cells reached confluence, Src inhibition had a small effect on Stat3 phosphorylation (Figure 5A, lane 4 vs. 10, and 5B, lane 5 vs. 9). This is in keeping with previous findings (Vultur *et al.*, 2004), indicating that the density-mediated, Stat3 activation is independent from Src function. In sharp contrast, these results also indicate that the Src kinase plays a significant role in the TAg-mediated, Stat3 phosphorylation.

To further examine the Src involvement in the TAg-mediated, Stat3 activation, we examined the ability of the SrcDN, dominant-negative mutant to prevent Stat3, tyr705 phosphorylation by TAg expression (see *Materials and Methods*; Hung and Elliott, 2001). This mutant was expressed in 10T½-TAg-1 cells through retroviral infection and puromycin-resistance selection, and Stat3-ptyr705 levels examined in sparsely growing cells. As a control, cells were infected with an empty pBabe-puro vector and selected for puromycin resistance in a similar manner. As shown in Figure 5C (lanes 1–4), SrcDN expression prevented the TAg-induced Stat3-ptyr705 phosphorylation. Furthermore, to examine the role of Src, as well as Fyn and Yes in the TAg-mediated, Stat3 phosphorylation we overexpressed the C-terminal Src kinase (Csk) gene through infection with the adenovirus vector pAdTrack (see *Materials and Methods*; Angers-Loustau *et al.*, 2004). This kinase phosphorylates all three Src family members on a COOH-terminal tyrosine, effectively inactivating these enzymes (Okada *et al.*, 1991). As a control, cells were infected with the same vector, but lacking the Csk insert. As shown in Figure 5C (lanes 5–8), Csk overexpression through infection with this vector caused a dramatic reduction in the Stat3-ptyr705 levels (lane 7 vs. 8), further confirming the role of Src in the TAg-mediated, Stat3 phosphorylation. Similar results were obtained with the SrcDN mutant, expressed with the adenovirus vector.

The role of the JAK kinases in the TAg-mediated, Stat3-tyr705 phosphorylation was examined next. TAg-expressing, 10T½-TAg-1 cells were grown to different densities and treated with the AG490 inhibitor previously shown to be selective for JAK at 50 $\mu$M (Zhang *et al.*, 2000), and Stat3-ptyr705 levels were examined as above. The specificity for JAK as opposed to Src kinases was monitored by examining FAK-861 phosphorylation levels as above. As shown in Figure 5D, AG490 treatment substantially reduced Stat3-ptyr705 levels, compared with control cells treated with the DMSO carrier alone. This inhibition was more pronounced at densities of <100% but was present even at postconfluence (lanes 1–5 vs. 6–10, Figure 5D), in agreement with previous results indicating that the density-dependent Stat3 activation is only partly blocked by AG490 treatment (Vultur *et al.*, 2004). The combination of PD180970 and AG490 caused a further inhibition (lanes 11–15), pointing to a synergistic effect between the Src and Jak kinases in Stat3 activation by TAg. As expected, Stat3 DNA binding activity paralleled the Stat3 phosphorylation levels. To examine the involvement of Jak2 specifically in the TAg-mediated, Stat3 activation, we used fibroblasts established from Jak2 knockout mice (see *Materials and Methods*). TAg was expressed in these cells and in their wild-type counterparts using the same retrovirus vector as above, and Stat3-ptyr705 phosphorylation examined in sparse cultures. As shown in Figure 5E, Stat3-ptyr705 phosphorylation was substantially lower in TAg-expressing, Jak2 null cells than their wild-type, TAg-expressing counterparts, indicating a role for Jak2 in the TAg-mediated, Stat3 activation.

A corollary to the concept that the JAK kinases may, at least in part, mediate Stat3 activation by TAg is that TAg increase JAK activity. To this effect, Jak1 and Jak2 in vitro kinase activity levels were examined in 10T½-TAg-1 cells (see *Materials and Methods*). As shown in Figure 5F, there was a dramatic increase in activity of both Jak1 and Jak2 kinases upon TAg expression, further reinforcing the conclusion that these kinases may at least in part mediate Stat3 phosphorylation in this system. At the same time, as expected, AG490 reduced Jak1 kinase activity indicating the effectiveness of the AG490 treatment at all densities examined (Figure 5F, top panel, lanes 5–8), whereas total Jak1 and Jak2 protein levels remained unaffected (unpublished data). These results taken together indicate that these JAK family kinases might be involved in mediating Stat3 phosphorylation in TAg-transformed cells, although they may not be solely responsible. On the other hand, in agreement with previous results indicating that the expression of Jak3 is restricted to the hematopoietic cell lineage (Johnston *et al.*, 1994; Witthuhn *et al.*, 1994), Jak3 activity levels were found to be very low both in the presence and absence of TAg; therefore, Jak3 is unlikely to be involved in the TAg-mediated, Stat3 phosphorylation in our fibroblast system. Similarly, treatment of cells with the Abl tyrosine kinase inhibitor, imatinib (Gleevec or STI-571; Nimmanapalli *et al.*, 2002; Daniels *et al.*, 2004) had no effect on Stat3 phosphorylation (Figure 5G, top panel, lanes 9–12 vs. 13–16), whereas no increase in c-Abl phosphorylation was observed upon TAg expression (Figure 5G, bottom panel, lanes 1–4 vs. 9–12). These results taken together indicate that the c-Abl kinase by itself is unlikely to be involved. In addition, no increase in c-Abl phosphorylation was observed with cell density in either 10T½ (Figure 5G, bottom panel, lanes 1–4), or 10T½-TAg-1 (Figure 5G, bottom panel, lanes 9–12) cells. Similarly, the Stat3 activation observed in pRb−/− cells was reduced through pharmacological inhibition of the Src or Jak kinases (Figure 5, H and I), but not Gleevec.

Previous results indicated that mouse embryo cells with a targeted disruption of the insulin-like growth factor-1 receptor (IGF1-R) cannot be transformed by TAg, indicating that IGF1-R is required for TAg-mediated transformation (Porcu *et al.*, 1994; Sell *et al.*, 1994; Fei *et al.*, 1995). IGF1-R is also known to activate Stat3 and to play a role in regulating cell-to-cell adhesion (Mauro *et al.*, 2003). To investigate whether the defect of IGF1R−/− cells in transformation by TAg was due at least partly to an inability to activate Stat3, TAg was expressed in cells with a targeted disruption of the IGF1R gene (IGFR−/− cells) and their wild-type counterparts, and Stat3-ptyr705 levels were examined as above. As shown in Figure 5J, the TAg-expressing, IGF1R−/− cells had substantially lower Stat3-ptyr705 levels than their wild-type counterparts (lanes 1–5 vs. 6–10), indicating that IGF1-R plays a significant role in the TAg-mediated Stat3 activation.

Fps/Fes and Fer are members of a distinct subfamily of nonreceptor protein-tyrosine kinases. Recent studies indicated that these kinases play a role in regulating cytoskeletal rearrangements and inside-out signaling that accompany receptor-ligand, cell-ECM, and cell-to-cell interactions (Greer, 2002). To examine whether the Fer kinase might be involved in the TAg-mediated, Stat3 phosphorylation, TAg was expressed in established cells derived from knockout mice, where this gene had been genetically ablated, and Stat3-ptyr705 levels were examined as above. As shown in

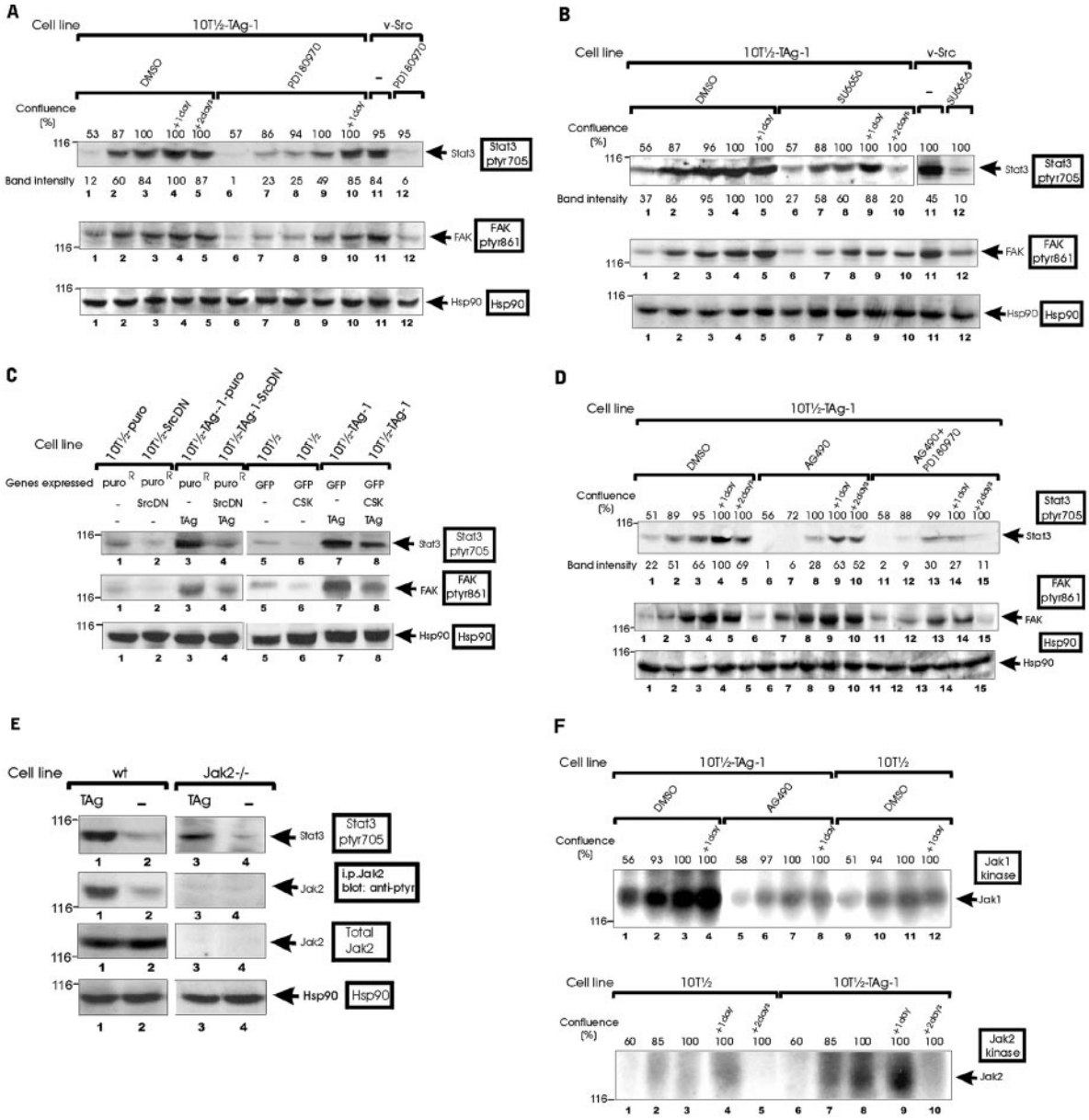


**Figure 5.** Src and Jak are required for Stat3 activation by TAg A-C: Src inhibition reduces TAg-mediated, Stat3 phosphorylation. (A) 10T½-TAg-1 fibroblasts were grown to different densities as indicated, with daily media changes and treated with the Src inhibitor PD180970 (lanes 6–10 and 12) or the DMSO diluent (lanes 1–5) for 24 h. Cell lysates were probed for Stat3-ptyr705 (top panel), FAK ptyr861 (middle panel), or Hsp90 (bottom panel) as a loading control. Lanes 11 and 12: v-Src–transformed NIH3T3 cells. Numbers under the lanes refer to band intensity values obtained through quantitation by fluorimager analysis, with the peak value of cells treated with the DMSO carrier alone taken as 100% (see *Materials and Methods*). (B) Same as in A, cells grown in the presence of the SU6656 Src inhibitor. (C) Dominant-negative Src or the C-terminal Src kinase reduce the TAg-mediated, Stat3-ptyr705 phosphorylation in subconfluent cells. Control, puromycin-resistant 10T½-puro (lane 1), or TAg-transformed, 10T½-TAg-puro (lane 3) cells, or their counterparts expressing the SrcDN mutant (lanes 2 and 4, respectively) were grown to 30% confluence, and cell lysates were probed for Stat3-ptyr705 (top panel), FAKptyr861 (middle panel), or Hsp90 (bottom panel) as a loading control, as indicated. Lanes 5–8: 10T½ or 10T½-TAg-1 cells were infected with the control pAdTrack (lanes 5 and 7) or the Ad-Csk vector containing the C-terminal Src kinase gene (lanes 6 and 8), respectively. Cell lysates were prepared 48 h later and probed for Stat3-ptyr705 (top panel), FAKptyr861 (middle panel), or Hsp90 (bottom panel) as a loading control, as indicated (see *Materials and Methods*). (D and E) Jak inhibition or genetic ablation reduces TAg-mediated, Stat3 phosphorylation. (D) 10T½-TAg-1 fibroblasts were grown to different densities as indicated, with daily media changes and treated with the Jak-selective inhibitor AG490 (lanes 6–10) or the DMSO diluent (lanes 1–5) or AG490 and PD180970 in combination (lanes 11–15), for 24 h. Cell lysates were probed for Stat3-ptyr705 (top panel), FAK ptyr861 (middle panel), or Hsp90 (bottom panel) as a control. Numbers under the lanes refer to band intensity values obtained through quantitation by fluorimager analysis, with the peak value of cells treated with the DMSO carrier alone taken as 100% (see *Materials and Methods*). (E) Jak2−/− cells (lanes 3 and 4) or cells from their wild-type littermates (lanes 1–2), before (lanes 2 and 4) or after (lanes (1 and 3) TAg expression were grown to 30% confluence, and cell extracts were probed for Stat3-ptyr705, total Jak2, or Hsp90 as a control, as indicated. Jak2 autophosphorylation was also measured by probing anti-Jak2 immunoprecipitates with an anti-phosphotyrosine antibody. (F) TAg expression leads to activation of the Jak1 and Jak2 kinases. Jak1 was immunoprecipitated from 10T½ (lanes 9–12) or 10T½-TAg-1 (lanes 1–8) cells grown to different densities as indicated and treated with the DMSO diluent (lanes 1–4 and 9–12) or AG490 (lanes 5–8), before the addition of 50 $\mu$Ci [$\gamma$-$^{32}$P]ATP, electrophoresis, and autoradiography (see *Materials and Methods*). Bottom panel: Jak2 was immunoprecipitated from control 10T½ (lanes 1–5) or 10T½-TAg-1 (lanes 6–10) cells grown to different densities as indicated, before the addition

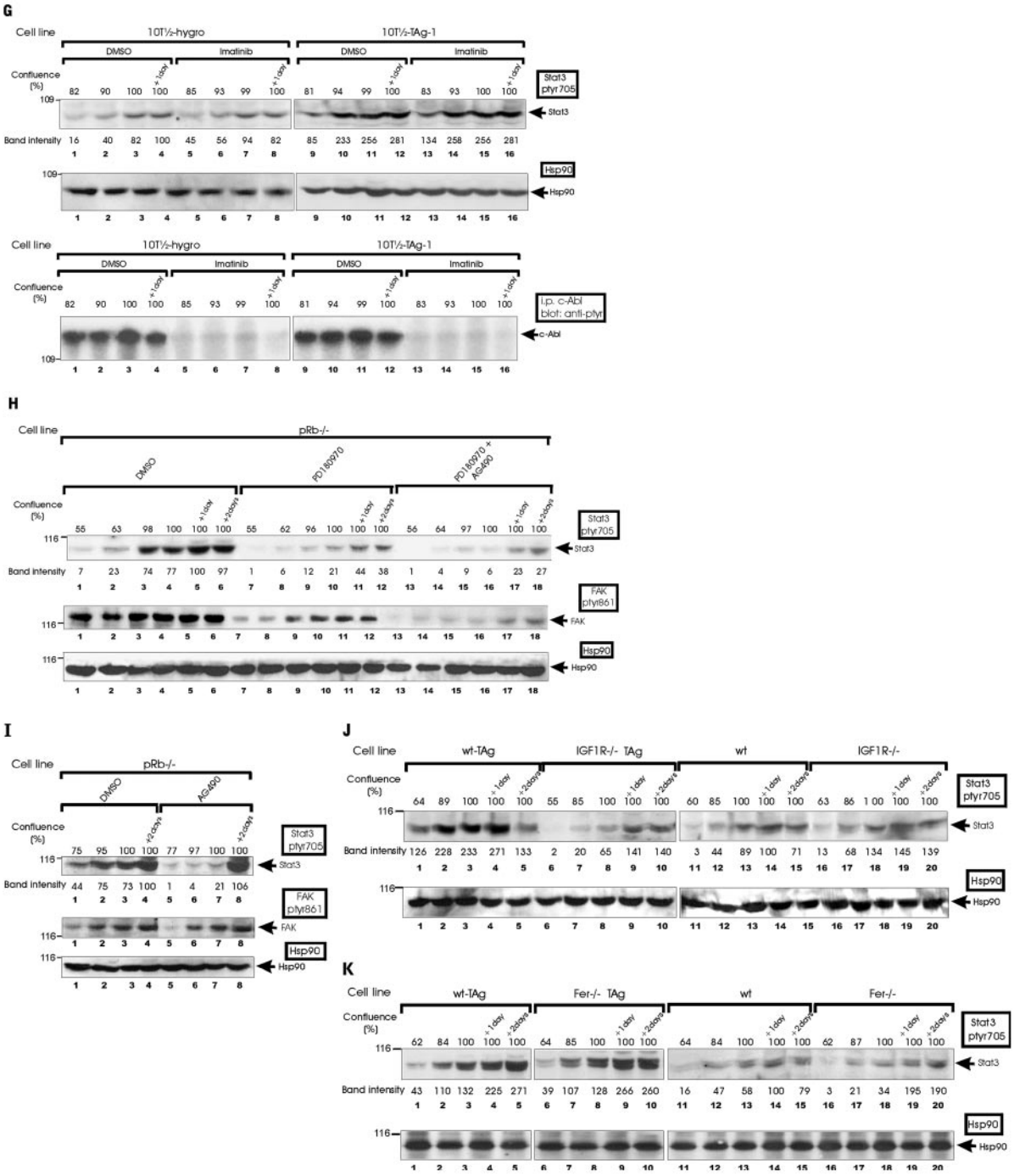


**Figure 5 (cont).** of 50 $\mu$Ci [$\gamma$-$^{32}$P]ATP, electrophoresis and autoradiography as above. (G) 10T½ (lanes 1–8) or 10T½-TAg-1 (9–16) fibroblasts were grown to different densities as indicated, with daily media changes and treated with the Abl inhibitor STI-571 (imatinib or Gleevec; lanes 5–8 and 13–16) or the DMSO diluent (lanes 1–4 and 9–12) for 48 h. Cell lysates were probed for Stat3-ptyr705 (top panel), or Hsp90 (middle panel) as a control. Arrows point to the position of Stat3-ptyr705 or Hsp90, respectively, as indicated. Bottom panel: the same extracts as in the top two panels were immunoprecipitated with an antibody to cAbl and blotted with an antibody against phosphotyrosine (see *Materials and Methods*). In the top panel, numbers under the lanes refer to band intensity values obtained through quantitation by fluorimager analysis, with the peak value of control 10T½-hygro cells treated with the DMSO carrier taken as 100% (see *Materials and Methods*). (H) Lysates from pRb−/− cells grown to different densities as indicated, with daily media changes and treated with the Src inhibitor PD180970 (lanes 7–12), or PD180970 and the Jak inhibitor AG490 (lanes 13–18), or the DMSO diluent (lanes 1–6) for 24 h. Cell lysates were probed for Stat3-ptyr705 (top panel), FAK ptyr861 (middle panel), or Hsp90 (bottom panel) as a loading control. Horizontal bars at the left refer to molecular-weight markers. Arrows point to the position of Stat3-ptyr705, FAK, or Hsp90, respectively, as indicated. In the top panel, numbers under the lanes refer to band intensity values obtained through quantitation by fluorimager analysis, with the peak value of cells treated with the DMSO carrier taken as 100% (see *Materials and Methods*). (I) Lysates from pRb−/− cells grown to different densities and treated with AG490 (lanes 5–8) or the DMSO carrier alone (lanes 1–4) were resolved by gel electrophoresis. Western immunoblots were probed for Stat3-ptyr705 (top panel), an activated form of the Src substrate FAK (FAK ptyr861, middle panel), or Hsp90 (bottompanel) as a control. Horizontal bars at the

**Figure 5 (cont).** left refer to molecular-weight markers. Arrows point to the position of Stat3-ptyr705, FAK, or Hsp90, respectively, as indicated. In the top panel, numbers under the lanes refer to band intensity values obtained through quantitation by fluorimager analysis, with the peak value of cells treated with the DMSO carrier taken as 100% (see *Materials and Methods*). (J) Cells established from mice with a targeted disruption of the IGF1R gene, before (lanes 16–20) or after (lanes 6–10) TAg expression were grown to different densities as indicated, and cell lysates were probed for Stat3-ptyr705. Lanes 1–5 and 11–15: cells from wild-type littermates, before (lanes 11–15) or after (lanes 1–5) TAg expression. In the top panel, numbers under the lanes refer to band intensity values obtained through quantitation by fluorimager analysis, with the peak value of control wild-type cells taken as 100% (see *Materials and Methods*). (K) Cells established from knockout mice where the Fer kinase was genetically ablated, before (lanes 16–20) or after (lanes 6–10) TAg expression, were grown to different densities as indicated, and cell lysates were probed for Stat3-ptyr705. Lanes 1–5 and 11–15: cells from wild-type littermates, before (11–15) or after (1–5) TAg expression. In the top panel, numbers under the lanes refer to band intensity values obtained through quantitation by fluorimager analysis, with the peak value of control wild-type cells taken as 100% (see *Materials and Methods*).

Figure 5K, Stat3-ptyr705 levels in the TAg-expressing, Fer−/− cells were indistinguishable from levels in their wild-type counterparts (lanes 1–5 vs. 6–10), indicating that the Fer kinase plays no significant role in the TAg-mediated Stat3 activation.

### *Stat3 Inhibition Induces Apoptosis of Confluent, TAg-transformed Cells*

Previous results have shown that Stat3 signaling induces the antiapoptotic *bcl-xL* and *mcl-1* genes, thus protecting tumor cells from apoptosis (Catlett-Falcone *et al.,* 1999; Grandis *et al.,* 2000; Epling-Burnette *et al.,* 2001). Because, as demonstrated above, Src is required for Stat3 activation by TAg, we examined the functional consequences of Src inhibition regarding apoptosis of TAg-transformed cells. 10T½ or 10T½-TAg-1 cells were treated with the PD180970 or SU6656 Src inhibitors at different densities, and apoptotic death was assessed by in situ TUNEL staining as well as by FACS analysis of the cellular sub-G1 profile (Vultur *et al.,* 2004). As shown in Figure 6A, Src inhibition with PD180970 induced apoptosis in 10T½-TAg-1 cells at densities of 60%, whereas there was little effect on the normal 10T½. Treatment with PD180970 was more effective than SU6656, consistent with its greater potency for Src kinase inhibition (Figure 5, A vs. B). However, both Src inhibitors were much less effective in 10T½-TAg-1 cells at time points beyond 100% confluence. This is in keeping with previous results indicating that the density-mediated, Stat3 activation in both normal and v-Src–transformed cells is independent from Src function (Vultur *et al.,* 2004) and indicates that Src inhibition cannot induce apoptosis in TAg-transformed cells in the face of extensive cell-cell contact. As expected, similar results were obtained with cells transformed by v-Src (Figure 6A, right panel).

Given that Src inhibition can block Stat3 activity only in subconfluent cells, we examined the functional consequences of direct Stat3 inhibition regarding apoptosis, at first by examining the phenotype of cells rendered constitutively Stat3 deficient through expression of a Stat3-specific, siRNA. 10T½, 10T½-si, 10T½-TAg-1, and 10T½-TAg-1-si cells were grown to different densities in plastic Petris, and apoptotic death was assessed as above. As shown in Figure 6B, very little apoptosis was observed in the parental 10T½ or control 10T½-TAg-1-U6 cells. However, apoptotic death was evident in sparse 10T½-TAg-1-si cells, and it dramatically increased to almost 100% by TUNEL staining at 1 d postconfluence, when Stat3-ptyr705 levels are normally at their highest. A similar increase in apoptotic death upon Stat3 down-regulation was observed with Cre expression in flox-SV-Cre-1 cells.

To more precisely examine the effect of Stat3 down-regulation expressly at the peak of Stat3 activity, upon apoptotic death induction in TAg-transformed cells, we made use of the cell-permeant, peptidomimetic inhibitor ISS610, which was previously demonstrated to block the Stat3-SH2 domain and inhibit Stat3 activity in vivo (Figure 6C, inset; Turkson *et al.,* 2004). As a control, we used a nonphosphorylated analog that is unable to bind the Stat3-SH2 domain (ISS610NP; Turkson *et al.,* 2004; see *Materials and Methods*). Cells were treated with the compounds at different densities for 24 h and then fixed, and apoptotic death was assessed. Same as the genetic methods of Stat3 down-regulation outlined above, ISS610 treatment caused a growth retardation of subconfluent 10T½ cells, reversed the transformed morphology, and abolished the ability of 10T½-TAg-1 cells to form foci overgrowing a monolayer of normal cells (unpublished data). Most importantly, as observed before using a peptide blocking the Stat3-SH2 domain (Vultur *et al.,* 2004), the degree of apoptosis induced by ISS610 in subconfluent, normal 10T½ cells was very low, whereas treatment at 1–3 d postconfluence resulted in a slight increase in apoptotic death (Figure 6C). On the other hand, Stat3 inhibition in TAg-transformed 10T½-TAg-1 cells induced apoptosis, which was much more dramatic in confluent cultures (Figure 6C). This is in sharp contrast to the PD180970 treatment, which was much more effective in subconfluent than confluent cells. At the same time, treatment with the inactive analog ISS610NP had no significant effect. The above results taken together indicate that direct inhibition of Stat3 signaling in TAg-transformed, mouse fibroblasts induces DNA degradation and apoptosis, which is especially pronounced in confluent cells, when Stat3 activity is at its highest. Inhibition of Src, however, although able to inhibit Stat3 activity and induce apoptosis in sparse cells, is ineffective in confluent cultures, possibly because of the fact that the cell-cell adhesion–mediated Stat3 activation is independent from Src function. Treatment with the AG490 JAK inhibitor also induced apoptosis, which at high densities was almost as pronounced as after inhibition of Stat3 with ISS610. This is consistent with previous observations indicating that at high densities Stat3-ptyr705 phosphorylation is partly JAK dependent (Vultur *et al.,* 2004).

## DISCUSSION

In this article we examined the potential role of Stat3 in transformation by TAg. The results demonstrated that Stat3 down-regulation through genetic manipulation or pharmacological inhibition caused a dramatic reduction in the cells' growth rate, focus formation ability, and anchorage-independence, consistent with a requirement for Stat3 activity in TAg-mediated transformation.

We previously demonstrated that cell-to-cell adhesion can exert a dramatic effect on Stat3 phosphorylation and activity in cultured normal or transformed cells (Vultur *et al.,* 2004). For this reason, to investigate TAg's potential for Stat3 activation, we examined Stat3 phosphorylation and activation levels at different densities of normal or TAg-transformed cells. Our findings indicate that TAg expression increases Stat3 phosphorylation, DNA binding and transcriptional activity even in sparsely growing cells with very low opportunity for cell-to-cell adhesion. This is further confirmed

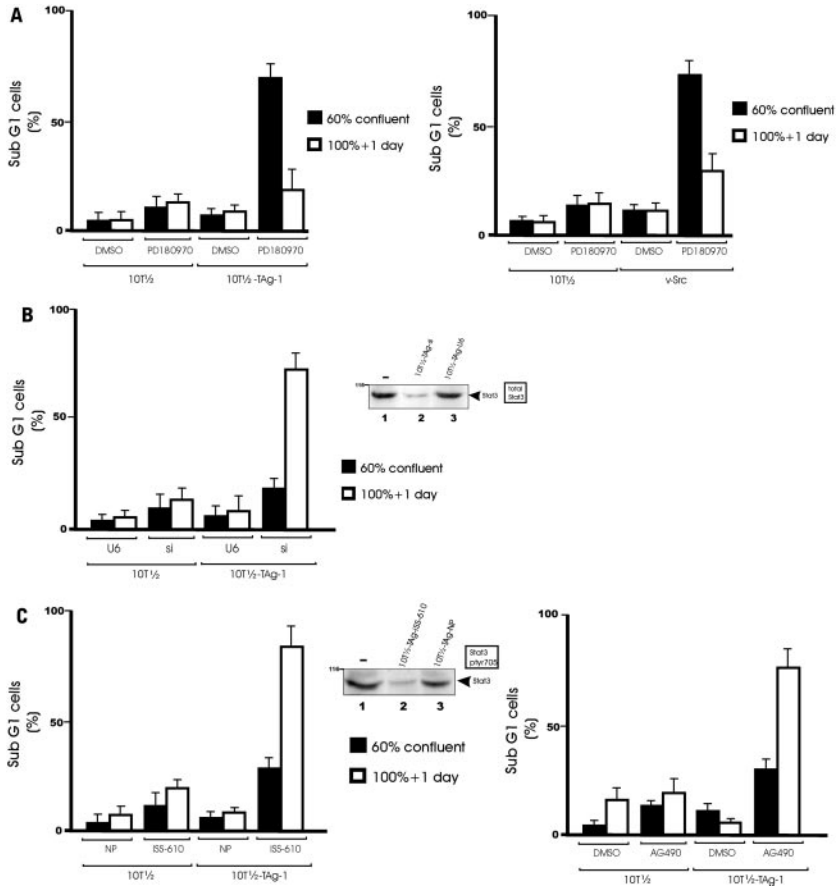


**Figure 6.** Stat3 inhibition can induce apoptosis of confluent, TAg-transformed cells. (A) Left panel: TAg-transformed, 10T½-TAg-1 cells, or the parental 10T½ were treated with the Src-selective inhibitor, PD180970, or the DMSO carrier for 24 h at 60% confluence, or 1 d postconfluence, fixed, stained with propidium iodide, and examined for apoptosis induction through sub-G1-profile analysis using a FACS flow cytometer. The results are averages ± SEM of three independent experiments. Right panel: v-Src–transformed, 10T½ cells and their normal counterparts, similarly treated. (B) The Stat3-specific, siRNA (si) was stably introduced in 10T½ cells or their TAg expressing counterparts, 10T½-TAg-1 (see *Materials and Methods*). Cells transfected with a vector lacking the siRNA insert served as controls (U6). Cells were fixed, stained with propidium iodide, and sub-G1 profile examined as above. The results are averages ± SEM of three independent experiments. Inset: examination of Stat3-ptyr705 levels by Western blotting in 10T½-TAg-1 cells transfected with a construct expressing siRNA (lane 2) or a control plasmid (lane 3). (C) Left panel: TAg-transformed, 10T½-TAg-1 cells, or the parental 10T½ were treated with the Stat3-specific peptidomimetic inhibitor, ISS610, or its inactive, nonphosphorylated analog, ISS610NP for 24 h at 60% confluence, or 1 d postconfluence, as indicated. Cells were then stained with propidium iodide and examined for apoptosis induction as above. The results are averages ± SEM of three independent experiments. Inset: examination of Stat3-ptyr705 levels by Western blotting in 10T½-TAg-1 cells treated with the ISS610 inhibitor (lane 2) or an inactive nonphosphorylated analog (lane 3). Right panel: TAg-transformed, 10T½-TAg-1 cells, or the parental 10T½ were treated with the JAK-selective inhibitor, AG490, or the DMSO diluent for 24 h at 60% confluence, or 1 d postconfluence, as indicated. Cells were then stained with propidium iodide and examined for apoptosis induction as above. The results are averages ± SEM of three independent experiments.

with studies using cultures where cell-cell contacts are abrogated through Calcium chelation, indicating that TAg per se has an intrinsic ability for Stat3 activation, independent from the increased opportunity for cell-to-cell adhesion brought about by transformation-induced, morphological changes. Therefore, albeit predominantly nuclear and thought to affect mostly nuclear targets, TAg requires the activity of Stat3, a signal transducer normally activated through phosphorylation by membrane tyrosine kinase receptors or oncogenes, to effect full neoplastic conversion.

An important TAg target is the pRb family of growth suppressors, pRb, p130, and p107 (Sullivan and Pipas, 2002). TAg expression inhibits pRb function and this interaction is required for transformation, even by cytoplasmic TAg mutants (Tedesco *et al.*, 1993). Current models of pRb function indicate that the upstream regulators of pRb activity (G1 cyclins, cyclin-dependent kinases, and their inhibitors) affect the phosphorylation status of pRb proteins and thereby their ability to bind to and regulate their best characterized targets, the E2F family of transcription factors, which are important cell cycle controllers (Trimarchi and Lees, 2002). Transcriptional activation by E2F is achieved either through active transactivation or derepression of genes having E2F-binding sites on their promoters. A detailed examination of E2F-activated genes by microarray analysis indicated that E2F1 has many targets, among which is a number of membrane receptor tyrosine kinases, including known Stat3 activators such as PDGFRα, IGF1R, VEGF, and others (Young *et al.*, 2003). In fact, it has long been demonstrated that TAg-transformed rodent fibroblasts secrete autocrine factors that enable the cells to proliferate when suspended in soft agar (Kaplan and Ozanne, 1982; Ciardiello *et al.*, 1990). Such an induction of growth factor or receptor genes by the E2F transcription factors after TAg expression would explain the observed Stat3 activation that might be needed to mediate signals generated in the producer cell by the autocrine loop. The fact that the pRb-binding site is required both for Stat3 activation and transformation by TAg stresses the importance of this pathway in TAg action. This conclusion is further reinforced by the fact that pRb inactivation through expression of adenovirus E1A or by genetic ablation also leads to Stat3 stimulation. Thus, although the possibility that TAg's interaction with other targets, such as the p53 antioncogene may contribute to Stat3 activation cannot be excluded (Lin *et al.*, 2002a, 2002b), it appears that pRb inactivation is an important factor in the TAg-mediated, Stat3 activation and neoplastic transformation.

Two other members of the pRb family have been extensively studied, p130 and p107 (Classon and Dyson, 2001). As with pRb, these family members also interact with E2F and repress the transcription of certain cell-cycle regulatory genes. In contrast to pRb, however, evidence that p130 or p107 are tumor suppressors, either in mouse or human cells is lacking. Our observation that unlike pRb−/−, p130- or p107-deficient cells did not display high Stat3 levels is in keeping with this finding. The observation that TAg expression, which binds to

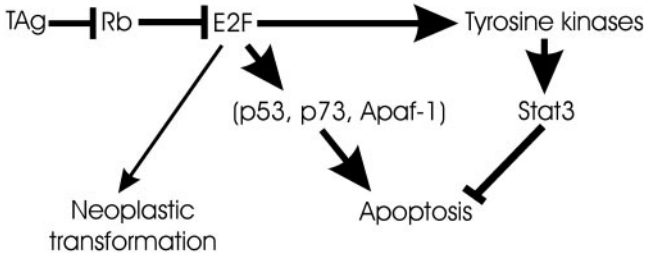


**Figure 7.** Role of Stat3 in transformation by TAg. TAg expression activates E2F through binding to and inactivation of pRb. E2F may then transcriptionally activate a number of kinases, such as IGF1-R or Src, which would activate Stat3, a potent apoptosis inhibitor. E2F can also induce apoptosis, through both p53-dependent and -independent mechanisms. Upon inhibition of Stat3 activity, TAg expression results in apoptosis (Sears and Nevins, 2002).

and inactivates all three pRb family members, or ablation of all three genes in cells from triple knockout mice, activates Stat3 indicates that the net result of inactivation of all three pRb family proteins is an increase in Stat3 activity.

The nature of the tyrosine kinase(s) potentially activated by TAg and responsible for Stat3 phosphorylation and activation is an interesting subject with important ramifications. Stimulation of a large number of receptors, such as growth factor receptors with intrinsic tyrosine kinase activity, as well as cytokine receptors lacking tyrosine kinase activity (e.g., IL6), is known to result in phosphorylation and activation of Stat3, mediated by the receptor tyrosine kinase itself and/or Jaks or Src (Yu and Jove, 2004). Our results, indicating that inhibition of the Src and Jak kinases in TAg expressing cells did reduce Stat3 phosphorylation, reveal that these kinases are indeed required for Stat3 phosphorylation after TAg transformation. In addition, targeted disruption of the IGF1-R gene had a dramatic effect on Stat3 activation by TAg. It is especially interesting to note in this respect that IGF1-R is one of the receptor kinases previously found to be transcriptionally up-regulated by E2F (Young *et al.*, 2003). Because IGF1-R could activate Src, it is possible that Stat3 may be downstream from the cascade E2F/IGF1R/Src/Stat3. On the other hand, Stat3 phosphorylation was not detectably affected by genetic ablation of another membrane tyrosine kinase receptor, Fer, in fibroblasts cultured from knockout mice, suggesting that this kinase by itself, which was not found to be an E2F target (Young *et al.*, 2003), does not play a significant role. We cannot however exclude the possibility that other tyrosine kinases may also be involved, at least in part, in the TAg-mediated Stat3 activation (Figure 7).

Our results further indicate that Stat3 activation by TAg may play an important role in preventing apoptosis, in addition to promoting growth and neoplastic transformation. It is especially remarkable that Stat3 inhibition could induce apoptosis of confluent, TAg-transformed cells. This is in sharp contrast to Src inhibition, which could induce apoptosis only in subconfluent, TAg-transformed cells. This could be due to the fact that the TAg-mediated, Stat3 activation is Src-dependent (Figure 5, A and B), whereas the density-mediated Stat3 activation is independent from Src action (Vultur *et al.*, 2004). The fact that direct Stat3 inhibition induces apoptosis very effectively in confluent cells, further underscores the importance of Stat3 in apoptosis inhibition, a finding that could have significant therapeutic implications. In any event, the present report presents evidence for Stat3 as an integral component of the signaling pathways from primarily nuclear, as well as membrane-bound oncogenes.

## ACKNOWLEDGMENTS

We are indebted to Dr. E. Parganas and Dr. J. Ihle for a gift of the Jak2 null cells and to Dr. D. R. Kaplan for the Src C-terminal kinase and Src-DN adenovirus vectors. We thank Dr. Mark Ewen and Dr. Tyler Jacks for gifts of the pRb family knockout cell lines, Dr. Daniel Links for the gifts of the Stat3C vectors, Dr. Thomas Roberts and Dr. Ole Gjoerup for gifts of the retroviral vectors expressing TAg mutants, Dr. Harvey Ozer for the tsA-transformed, human fibroblasts, Dr. Peter Greer and Dr. Andrew Craig for Fer−/− cells, Dr. Elisabeth Buchdunger of Novartis Pharma AG (Basel, Switzerland) for a generous gift of the Gleevec inhibitor, Dr. Bruce Elliott for the Src-DN retroviral vector and advice on cell-to-cell adhesion signaling, Dr. Erik Schaefer for many helpful discussions, and Dr. Mark Ewen for a critical reading of the manuscript. We also thank Marilyn Garrett and Chris Knight for very enthusiastic technical assistance. A.V. was supported by studentships from the Natural Sciences and Engineering Research Council of Canada (NSERC), the Ontario graduate studentship program and a Queen's University Graduate Award (QGA). R.A. was supported by a studentship from the Canadian Institutes of Health Research (CIHR), a predoctoral traineeship award from the Department of Defense Breast Cancer Research Program (BCRP-CDMRP), and a QGA. The financial assistance of CIHR, the Canadian Breast Cancer Research Alliance, the Cancer Research Society Inc., and NSERC through grants to L.R. is gratefully acknowledged.

## REFERENCES

Akira, S. (2000). Roles of STAT3 defined by tissue-specific gene targeting. Oncogene *19*, 2607–2611.

Angers-Loustau, A., Hering, R., Werbowetski, T. E., Kaplan, D. R., and Del Maestro, R. F. (2004). SRC regulates actin dynamics and invasion of malignant glial cells in three dimensions. Mol. Cancer Res. *2*, 595–605.

Arulanandam, R., Vultur, A., and Raptis, L. (2005). Transfection techniques affecting Stat3 activity levels. Anal. Biochem. *338*, 83–89.

Bromberg, J. F., Horvath, C. M., Besser, D., Lathem, W. W., and Darnell, J. E., Jr. (1998). Stat3 activation is required for cellular transformation by v-src. Mol. Cell. Biol. *18*, 2553–2558.

Bromberg, J. F., Wrzeszczynska, M. H., Devgan, G., Zhao, Y., Pestell, R. G., Albanese, C., and Darnell, J. E., Jr. (1999). Stat3 as an oncogene. Cell *98*, 295–303.

Calalb, M. B., Zhang, X., Polte, T. R., and Hanks, S. K. (1996). Focal adhesion kinase tyrosine-861 is a major site of phosphorylation by Src. Biochem. Biophys. Res. Commun. *228*, 662–668.

Catlett-Falcone, R. *et al.* (1999). Constitutive activation of Stat3 signaling confers resistance to apoptosis in human U266 myeloma cells. Immunity *10*, 105–115.

Chau, B. N., and Wang, J. Y. (2003). Coordinated regulation of life and death by RB. Nat. Rev. Cancer *3*, 130–138.

Ciardiello, F., Valverius, E. M., Colucci-D'Amato, G. L., Kim, N., Bassin, R. H., and Salomon, D. S. (1990). Differential growth factor expression in transformed mouse NIH-3T3 cells. J. Cell Biochem. *42*, 45–57.

Cirri, P., Chiarugi, P., Marra, F., Raugei, G., Camici, G., Manao, G., and Ramponi, G. (1997). c-Src activates both STAT1 and STAT3 in PDGF-stimulated NIH3T3 cells. Biochem. Biophys. Res. Commun. *239*, 493–497.

Classon, M., and Dyson, N. (2001). p107 and p130, versatile proteins with interesting pockets. Exp. Cell Res. *264*, 135–147.

Daniels, C. E., Wilkes, M. C., Edens, M., Kottom, T. J., Murphy, S. J., Limper, A. H., and Leof, E. B. (2004). Imatinib mesylate inhibits the profibrogenic activity of TGF-beta and prevents bleomycin-mediated lung fibrosis. J. Clin. Invest. *114*, 1308–1316.

Epling-Burnette, P. K. *et al.* (2001). Inhibition of STAT3 signaling leads to apoptosis of leukemic large granular lymphocytes and decreased Mcl1 expression. J. Clin. Invest. *107*, 351–362.

Fei, Z. L., D'Ambrosio, C., Li, S., Surmacz, E., and Baserga, R. (1995). Association of insulin receptor substrate 1 with simian virus 40 large T antigen. Mol. Cell. Biol. *15*, 4232–4239.

Gabarra-Niecko, V., Schaller, M. D., and Dunty, J. M. (2003). FAK regulates biological processes important for the pathogenesis of cancer. Cancer Metastasis Rev. *22*, 359–374.

Garcia, R. *et al.* (2001). Constitutive activation of Stat3 by the Src and JAK tyrosine kinases participates in growth regulation of human breast carcinoma cells. Oncogene *20*, 2499–2513.

Grammatikakis, N. *et al.* (2001). Simian Virus 40 large Tumor antigen modulates the Raf signaling pathway. J. Biol. Chem. *276*, 27840–27845.

Grammatikakis, N., Vultur, A., Ramana, C. V., Siganou, A., Schweinfest, C. W., and Raptis, L. (2002). The role of Hsp90N, a new member of the Hsp90 family, in signal transduction and neoplastic transformation. J. Biol. Chem. *277*, 8312–8320.

Grandis, J. R., Drenning, S. D., Zeng, Q., Watkins, S. C., Melhem, M. F., Endo, S., Johnson, D. E., Huang, L., He, Y., Kim, J. D. (2000). Constitutive activation of Stat3 signaling abrogates apoptosis in squamous cell carcinogenesis in vivo. Proc. Natl. Acad. Sci. USA *97*, 4227–4232.

Greer, P. (2002). Closing in on the biological functions of Fps/Fes and Fer. Nat. Rev. Mol. Cell Biol. *3*, 278–289.

He, T. C., Zhou, S., da Costa, L. T., Yu, J., Kinzler, K. W., and Vogelstein, B. (1998). A simplified system for generating recombinant adenoviruses. Proc. Natl. Acad. Sci. USA *95*, 2509–2514.

Huang, M. *et al.* (2002). Inhibition of Bcr-Abl kinase activity by PD180970 blocks constitutive activation of Stat5 and growth of CML cells. Oncogene *21*, 8804–8816.

Hung, W., and Elliott, B. (2001). Co-operative effect of c-Src tyrosine kinase and Stat3 in activation of hepatocyte growth factor expression in mammary carcinoma cells. J. Biol. Chem. *276*, 12395–12403.

Johnston, J. A., Kawamura, M., Kirken, R. A., Chen, Y. Q., Blake, T. B., Shibuya, K., Ortaldo, J. R., McVicar, D. W., and O'Shea, J. J. (1994). Phosphorylation and activation of the Jak-3 Janus kinase in response to interleukin-2. Nature *370*, 151–153.

Kaplan, P. L., and Ozanne, B. (1982). Polyoma virus transformed cells produce transforming growth factors and grow in serum-free medium. Virology *123*, 372–380.

Levy, D. E., and Darnell, J. E., Jr. (2002). Stats: transcriptional control and biological impact. Nat. Rev. Mol. Cell Biol. *3*, 651–662.

Lin, J., Jin, X., Rothman, K., Lin, H. J., Tang, H., and Burke, W. (2002a). Modulation of signal transducer and activator of transcription 3 activities by p53 tumor suppressor in breast cancer cells. Cancer Res. *62*, 376–380.

Lin, J., Tang, H., Jin, X., Jia, G., and Hsieh, J. T. (2002b). p53 regulates Stat3 phosphorylation and DNA binding activity in human prostate cancer cells expressing constitutively active Stat3. Oncogene *21*, 3082–3088.

Mauro, L., Salerno, M., Morelli, C., Boterberg, T., Bracke, M. E., and Surmacz, E. (2003). Role of the IGF-I receptor in the regulation of cell-cell adhesion: implications in cancer development and progression. J. Cell Physiol. *194*, 108–116.

McLemore, M. L., Grewal, S., Liu, F., Archambault, A., Poursine-Laurent, J., Haug, J., and Link, D. C. (2001). STAT-3 activation is required for normal G-CSF-dependent proliferation and granulocytic differentiation. Immunity *14*, 193–204.

Narimatsu, M. *et al.* (2001). Tissue-specific autoregulation of the stat3 gene and its role in interleukin-6-induced survival signals in T cells. Mol. Cell. Biol. *21*, 6615–6625.

Nimmanapalli, R., O'Bryan, E., Huang, M., Bali, P., Burnette, P. K., Loughran, T., Tepperberg, J., Jove, R., Bhalla, K. (2002). Molecular characterization and sensitivity of STI-571 (imatinib mesylate, Gleevec)-resistant, Bcr-Abl-positive, human acute leukemia cells to SRC kinase inhibitor PD180970 and 17-allylamino-17-demethoxygeldanamycin. Cancer Res. *62*, 5761–5769.

Okada, M., Nada, S., Yamanashi, Y., Yamamoto, T., and Nakagawa, H. (1991). CSK: a protein-tyrosine kinase involved in regulation of src family kinases. J. Biol. Chem. *266*, 24249–24252.

Olayioye, M. A., Beuvink, I., Horsch, K., Daly, J. M., and Hynes, N. E. (1999). ErbB receptor-induced activation of stat transcription factors is mediated by Src tyrosine kinases. J. Biol. Chem. *274*, 17209–17218.

Porcu, P., Grana, X., Li, S., Swantek, J., De Luca, A., Giordano, A., Baserga, R. (1994). An E2F binding sequence negatively regulates the response of the insulin-like growth factor 1 (IGF-I) promoter to simian virus 40T antigen and to serum. Oncogene *9*, 2125–2134.

Radna, R. L., Canton, Y., Jha, K. K., Kaplan, P., Li, G., Tranganos, R., and Ozer, H. L. (1989). Growth of immortalized Simian Virus 40 tsA-transformed human fibroblasts is temperature dependent. Mol. Cell. Biol. *9*, 3093–3096.

Raptis, L., Brownell, H. L., Vultur, A. M., Ross, G., Tremblay, E., and Elliott, B. E. (2000). Specific inhibition of growth factor-stimulated ERK1/2 activation in intact cells by electroporation of a Grb2-SH2 binding peptide. Cell Growth Differ. *11*, 293–303.

Raptis, L., Brownell, H. L., Wood, K., Corbley, M., Wang, D., and Haliotis, T. (1997a). Cellular ras gene activity is required for full neoplastic transformation by Simian Virus 40. Cell Growth Differ. *8*, 891–901.

Raptis, L., Lamfrom, H., and Benjamin, T. L. (1985). Regulation of cellular phenotype and expression of polyomavirus middle T antigen in rat fibroblasts. Mol. Cell. Biol. *5*, 2476–2486.

Raptis, L., Yang, J., Brownell, H. L., Lai, J., Preston, T., Corbley, M. J., Narsimhan, R. P., and Haliotis, T. (1997b). $Ras^{leu61}$ blocks differentiation of transformable 3T3 L1 and C3HT1/2derived preadipocytes in a dose- and time-dependent manner. Cell Growth Differ. *8*, 11–21.

Rothen-Rutishauser, B., Riesen, F. K., Braun, A., Gunthert, M., and Wunderli-Allenspach, H. (2002). Dynamics of tight and adherens junctions under EGTA treatment. J. Membr. Biol. *188*, 151–162.

Sage, J., Mulligan, G. J., Attardi, L. D., Miller, A., Chen, S., Williams, B., Theodorou, E., and Jacks, T. (2000). Targeted disruption of the three Rb-related genes leads to loss of G(1) control and immortalization. Genes Dev. *14*, 3037–3050.

Sears, R. C., and Nevins, J. R. (2002). Signaling networks that link cell proliferation and cell fate. J. Biol. Chem. *277*, 11617–11620.

Sell, C., Dumenil, G., Deveaud, C., Miura, M., Coppola, D., DeAngelis, T., Rubin, R., Efstratiadis, A., and Baserga, R. (1994). Effect of a null mutation of the insulin-like growth factor I receptor gene on growth and transformation of mouse embryo fibroblasts. Mol. Cell. Biol. *14*, 3604–3612.

Sullivan, C. S., and Pipas, J. M. (2002). T antigens of simian virus 40, molecular chaperones for viral replication and tumorigenesis. Microbiol. Mol. Biol. Rev. *66*, 179–202.

Tedesco, D., Fischer-Fantuzzi, L., and Vesco, C. (1993). Limits of transforming competence of SV40 nuclear and cytoplasmic large T mutants with altered Rb binding sequences. Oncogene *8*, 549–557.

Trimarchi, J. M., and Lees, J. A. (2002). Sibling rivalry in the E2F family. Nat. Rev. Mol. Cell Biol. *3*, 11–20.

Turkson, J., Bowman, T., Garcia, R., Caldenhoven, E., de Groot, R. P., and Jove, R. (1998). Stat3 activation by Src induces specific gene regulation and is required for cell transformation. Mol. Cell. Biol. *18*, 2545–2552.

Turkson, J., Kim, J. S., Zhang, S., Yuan, J., Huang, M., Glenn, M., Haura, E., Sebti, S., Hamilton, A. D., and Jove, R. (2004). Novel peptidomimetic inhibitors of signal transducer and activator of transcription 3 dimerization and biological activity. Mol. Cancer Ther. *3*, 261–269.

Turkson, J., Ryan, D., Kim, J. S., Zhang, Y., Chen, Z., Haura, E., Laudano, A., Sebti, S., Hamilton, A. D., and Jove, R. (2001). Phosphotyrosyl peptides block Stat3-mediated DNA binding activity, gene regulation, and cell transformation. J. Biol. Chem. *276*, 45443–45455.

Vignais, M. L., and Gilman, M. (1999). Distinct mechanisms of activation of Stat1 and Stat3 by PDGF receptor in a cell-free system. Mol. Cell. Biol. *19*, 3727–3735.

Vignais, M. L., Sadowski, H. B., Watling, D., Rogers, N. C., and Gilman, M. (1996). PDGF induces phosphorylation of multiple JAK family kinases and STAT proteins. Mol. Cell. Biol. *16*, 1759–1769.

Vultur, A., Cao, J., Arulanandam, R., Turkson, J., Jove, R., Greer, P., Craig, A., Elliott, B. E., and Raptis, L. (2004). Cell to cell adhesion modulates Stat3 activity in normal and breast carcinoma cells. Oncogene *23*, 2600–2616.

Wagner, B. J., Hayes, T. E., Hoban, C. J., and Cochran, B. H. (1990). The SIF binding element confers sis/platelet-derived growth factor inducibility onto the c-fos promoter. EMBO J. *9*, 4477–4484.

Wang, Y. Z., Wharton, W., Garcia, R., Kraker, A., Jove, R., and Pledger, W. J. (2000). Activation of Stat3 preassembled with PDGF beta receptors requires Src kinase activity. Oncogene *19*, 2075–2085.

Witthuhn, B. A., Silvennoinen, O., Miura, O., Lai, K. S., Cwik, C., Liu, E. T., and Ihle, J. N. (1994). Involvement of the Jak-3 Janus kinase in signalling by interleukins 2 and 4 in lymphoid and myeloid cells. Nature *370*, 153–157.

Young, A. P., Nagarajan, R., and Longmore, G. D. (2003). Mechanisms of transcriptional regulation by Rb-E2F segregate by biological pathway. Oncogene *22*, 7209–7217.

Yu, C. L., Meyer, D. J., Campbell, G. S., Larner, A. C., Carter-Su, C., Schwartz, J., and Jove, R. (1995). Enhanced DNA-binding activity of a Stat3-related protein in cells transformed by the Src oncoprotein. Science *269*, 81–83.

Yu, H., and Jove, R. (2004). The STATs of cancer—new molecular targets come of age. Nat. Rev. Cancer *4*, 97–105.

Zalvide, J., Stubdal, H., and DeCaprio, J. A. (1998). The J domain of Simian Virus 40 Large Tumor antigen is required to functionally inactivate Rb family proteins. Mol. Cell. Biol. *18*, 1408–1415.

Zhang, Y., Turkson, J., Carter-Su, C., Smithgall, T., Levitzki, A., Kraker, A., Krolewski, J. J., Medveczky, P., and Jove, R. (2000). Activation of Stat3 in v-Src transformed fibroblasts requires cooperation of Jak1 kinase activity. J. Biol. Chem. *275*, 24935–24944.